HHS Public Access

Author manuscript

Sci Immunol. Author manuscript; available in PMC 2022 September 10.

Published in final edited form as:

Sci Immunol. 2021 September 10; 6(63): eabh3034. doi:10.1126/sciimmunol.abh3034.

PD-1 blockade and vaccination provide therapeutic benefit against SIV by inducing broad and functional CD8+ T cells in lymphoid tissue

Sheikh Abdul Rahman[1,2,†], **Bhrugu Yagnik**[1,2,†], **Alexander P. Bally**[1,2], **Kristen N. Morrow**[1,2], **Shelly Wang**[1], **Thomas H. Vanderford**[1], **Gordon J. Freeman**[3,4], **Rafi Ahmed**[1,2], **Rama Rao Amara**[1,2,*]

[1]Division of Microbiology and Immunology, Emory Vaccine Centre, Yerkes National Primate Research Centre, Emory University, Atlanta, Georgia, USA.

[2]Department of Microbiology and Immunology, Emory School of Medicine, Emory University, Atlanta, Georgia, USA.

[3]Department of Medical Oncology and Cancer Vaccine Centre, Dana-Farber Cancer Institute, Boston, Massachusetts, USA.

[4]Harvard Medical School, Boston, Massachusetts, USA.

Abstract

During antiretroviral therapy (ART), most of the human immunodeficiency virus (HIV) reservoirs persist in the B cell follicles (BCFs) of lymphoid tissue. Thus, for HIV cure strategies, it is critical to generate cytolytic CD8+ T cells that home to BCF, reduce the reservoir burden, and maintain strong antiviral responses in the absence of ART. Here, using a chronic simian immunodeficiency virus (SIV)/rhesus macaque model, we showed that therapeutic vaccination under ART using a CD40L plus TLR7 agonist–adjuvanted DNA/modified vaccinia Ankara vaccine regimen induced robust and highly functional, SIV-specific CD4+ and CD8+ T cell responses. In addition, the vaccination induced SIV-specific CD8+ T cells in the lymph nodes (LNs) that could home to BCF. Administration of PD-1 blockade before initiation of ART and during vaccination markedly increased the frequency of granzyme B+ perforin+ CD8+ T cells in the blood and LN, enhanced their localization in germinal centers of BCF, and reduced the viral reservoir. After ART interruption, the vaccine + anti–PD-1 antibody–treated animals, compared with the vaccine alone and ART alone control animals, displayed preservation of the granzyme B+ CD8+ T cells

[*]**Correspondence:** Correspondence should be addressed to Dr. Rama Amara. Phone: (404) 727-8765; FAX: (404) 727-7768; ramara@emory.edu.

Author contributions: S.A.R. and B.Y. designed research, performed research, analyzed and interpreted the data, and wrote the manuscript. A.P.B. and K.N.M. designed research, performed research. S.W. performed qPCR analyses of SIV RNA and DNA in monkey samples. T.H.V. supervised the qPCR analyses of SIV RNA and DNA in monkey samples. G.J.F. synthesized primatized PD-1 mAb and provided helpful discussions regarding the study design. R.R.A. conceived the study. R.A. and R.R.A. designed the research and interpreted data throughout the study. R.R.A. supervised the research and wrote the manuscript.

[†]Equal contributions

Competing interests: R.A., G.J.F., and R.R.A. are co-inventors of PD-1 technology that has been licensed to Genentech by Emory University. G.J.F. has patents/pending royalties on the PD-1/PD-L1 pathway from Roche, Merck MSD, Bristol-Myers-Squibb, Merck KGA, Boehringer-Ingelheim, AstraZeneca, Dako, Leica, Mayo Clinic, and Novartis. G.J.F. has served on advisory boards for Roche, Bristol-Myers-Squibb, Xios, Origimed, Triursus, iTeos, NextPoint, IgM, Jubilant, and GV20. G.J.F. has equity in Nextpoint, Triursus, Xios, iTeos, IgM, and GV20. The other authors declare that they have no competing interests.

in the T cell zone and BCF of LN, maintained high SIV antigen-recognition breadth, showed control of reemerging viremia, and improved survival. Our findings revealed that PD-1 blockade enhanced the therapeutic benefits of SIV vaccination by improving and sustaining the function and localization of vaccine-induced CD8+ T cells to BCF and decreasing viral reservoirs in lymphoid tissue. This work has potential implications for the development of curative HIV strategies.

INTRODUCTION

Chronic HIV/simian immunodeficiency virus (SIV) infection depletes CD4+ T cells and erodes CD8+ T cell cytolytic potential by making them dysfunctional, a state known as exhaustion that is marked by the overexpression of programmed death-1 (PD-1) (1–4). Chronic HIV infection also causes persistent immune activation leading to a heightened inflammatory state, resulting in severe dampening of immune responses (5). Although antiretroviral therapy (ART) controls HIV/SIV viral infection and prevents infection of new CD4+ cells, it cannot clear the latently infected CD4+ T cells (viral reservoirs) that are responsible for rapid viral rebound after analytical treatment interruption (ATI) (6–10). The ART also fails to completely resolve chronic inflammation, resulting in suboptimal immune reconstitution (11, 12). Furthermore, a considerable fraction of the viral reservoir is confined to B cell follicles (BCFs), necessitating the generation of antiviral CD8+ T cells that can home to the BCF (8, 13–17). HIV-specific CD8+ T cells during chronic infection are largely excluded from the BCF (18, 19), and we previously showed that higher expression of the chemokine receptor CXCR5, required for homing to BCF, on SIV-specific CD8+ T cells associates with enhanced viral control during chronic SIV infection (20). Thus, there is a need to develop new HIV cure strategies that can induce highly functional virus-specific CD4+ and CD8+ T cells under ART and enhance homing of SIV-specific CD8+ T cells with killing potential to BCFs, in addition to reducing viral reservoirs. Therefore, facilitating the homing of highly functional CD8+ T cells into the BCF represents a promising therapeutic strategy.

PD-1 blockade during chronic SIV infection can improve CD8+ T cell functions (21, 22). Furthermore, administration of anti–PD-1 antibody before initiation of ART and during ART potentiates the latent reservoir reduction in rhesus macaques (RMs) chronically infected with SIV (23). However, PD-1 blockade during ART does not significantly increase the magnitude of antiviral T cell immunity highlighting the need for combining PD-1 blockade with therapies that can induce strong antiviral T cell response and potentiate BCF homing of CD8+ T cell with broad and potent antiviral functions. A possible strategy would be combining PD-1 blockade with therapeutic vaccination, which can potentially achieve two key goals toward a functional HIV cure: (i) PD-1 blockade would rejuvenate CD8 T cells that are functionally exhausted during chronic infection in addition to reducing viral reservoirs under ART, and (ii) vaccination would induce potent and broad antiviral T cell responses with the potential to home to BCF. Toward this, studies that combined vaccination with the PD-1 blockade have shown promising results in cancer studies (24–26) and in the lymphocytic choriomeningitis virus (LCMV) infection model (27). These findings have generated profound interest in combining therapeutic vaccination with the PD-1 checkpoint blockade as an HIV treatment strategy.

Here, we studied the therapeutic potential of vaccination using a combination of CD40L and Toll-like receptor 7 (TLR7) agonist– adjuvanted DNA prime/modified vaccinia Ankara (MVA) boost approach (28, 29) in the presence or absence of PD-1 immune checkpoint blockade in chronically SIV-infected RMs under ART. Specifically, we wanted to assess the combined effect of vaccination and PD-1 blockade on the following: (i) induction of broad and potent antiviral immunity, (ii) localization of cytotoxic CD8+ T cells into lymphoid tissue, (iii) reduction of viral reservoirs in lymph node (LN), and (iv) the impact on rebounding viremia after ATI. Therapeutic vaccination under ART induced a broad and highly functional SIV-specific CD4+ and CD8+ T cell response, and vaccine-induced SIV-specific CD8+ T cells expressed granzyme B (GrzB) and homed to the BCF in both vaccine groups. However, compared with vaccination alone, vaccination plus anti–PD-1 therapy reduced viral reservoirs in LNs during ART and preserved the magnitude, SIV antigen recognition breadth, and BCF homing of the antiviral CD8+ T cell response after ART interruption. This preservation of CD8+ T cell function was associated with better control of rebounding viremia and survival after ART interruption. These results highlight the potential of a combination strategy involving the vaccination and anti–PD-1 therapy to improve and sustain the functional CD8+ T cell response, thus reducing viral reservoirs in the lymphoid tissues during chronic SIV infection.

RESULTS

Study design

To study the influence of PD-1 blockade on therapeutic vaccination under ART, we infected three groups of RMs with SIVmac239 intrarectally to induce chronic infection and initiated ART at 10 weeks after infection (Fig. 1A). Two groups were subsequently immunized with a CD40L plus TLR7 agonist–adjuvanted DNA/MVA SIV239 vaccine, one without (vaccine-only, n = 6) and the other with anti– PD-1 therapy (vaccine + PD-1, n = 7). The third group did not receive vaccination or anti–PD-1 therapy and served as the ART-only control group (control, n = 6) (table S1). Vaccination consisted of two intradermal DNA/SIV239-CD40L vaccine primes followed by two intramuscular (IM) MVA/SIV239 vaccine boosts at 4-week intervals starting at week 38 (28 weeks after ART initiation) except for the last MVA boost, which was given 14 weeks after the first MVA boost. The DNA vaccine expressed SIV239 Gag, Pol, envelope (gp160), Tat, Rev, and membrane-anchored macaque CD40L. The MVA vaccine expressed SIV239 Gag, Pol, and envelope (gp150). Both vaccine groups also received ectopic application of imiquimod (a TLR7 agonist) cream as an adjuvant at 6 and 24 hours after each DNA vaccination because a combination of TLR7 and CD40 signaling induces potent CD8+ T cell responses in the absence of CD4+ T cell help (30, 31). Further, TLR7 agonist could also act as a latency reversal agent (LRA) as has been shown when delivered orally (32). However, we do not know whether it can be used as an LRA when used topically. To test this, four applications of imiquimod were given starting from 2 weeks after the first MVA boost, and two applications were given starting from 2 weeks after the second MVA boost with 2-week interval between each application.

The vaccine + PD-1 group received primatized anti–PD-1 treatment in two phases as previously described when testing the therapeutic benefits of PD-1 blockade combined with

ART (23). The first phase (referred to as phase 1 henceforth) consisted of five doses on days 0, 3, 7, 10, and 14 at 3 mg/kg starting 10 days before the initiation of ART. The second phase (referred to as phase 2 henceforth) consisted of three 10 mg/kg doses every 3 weeks starting with the first DNA prime during ART. The goals for the first phase were (i) to restore the function of dysfunctional CD8+ T cell response by PD-1 blockade during chronic viral replication in the absence of ART and (ii) that these functional CD8+ T cells will work synergistically with ART to clear virus-infected CD4+ T cells when ART is initiated. Using this approach, we previously showed that the virus pulldown was significantly faster (42 days versus 150+ days) in the ART + PD-1 group compared with ART-only group (23). We also observed that PD-1 blockade during ART does not significantly improve T cell function in blood (23). Thus, one of the primary goals for using PD-1 blockade plus vaccination during ART was to see whether it could further enhance the magnitude and breadth of T cell response induced by vaccination. This was based on the previous studies showing that PD-1 blockade during acute LCMV infection in mice (33) and vaccination in macaques (22) increases the magnitude of CD8+ T cell responses. In addition, we proposed that the LRA function of PD-1 blockade as shown by us and others (23, 34) reactivates virus in some fraction of latently infected cells, and these virus-reactivated CD4+ T cells will be killed by the functional CD8+ T cells potentially leading to lower viral reservoirs.

Here, we did not observe a significant impact of PD-1 blockade during the phase 1 on viral suppression or CD8 T cell proliferation (fig. S1, A to C), and we elaborated on possible reasons for this in Discussion. In addition, PD-1 blockade during the initiation of ART and DNA vaccinations resulted in the generation of antidrug antibodies (ADA), and thus we did not continue PD-1 blockade during MVA vaccinations (fig. S1D). The induction of ADA during phase 2 was associated with poor receptor occupancy of PD-1 on T cells (fig. S1E); however, it did not influence the proliferative capability of CD8+ T cells that was observed at 1 week after blockade (fig. S1F). Furthermore, ADA did not affect the induction cytolytic markers on CD8+ T cells (fig. S1G). All vaccinations were carried out under complete viral suppression by ART (Fig. 1B and fig. S2, A to C). ATI was performed at week 66 (6 weeks after the second MVA boost), and RMs were followed for 26 weeks after ATI to check for viral rebound, development of AIDS, and survival.

Combination of PD-1 blockade and vaccination enhanced the frequency and persistence of GrzB+ perforin+ CD8+ T cells in blood

DNA prime and MVA boost vaccination under ART induced expansion of CD8+ T cells in both vaccine-only and vaccine + PD-1 groups as marked by increase in Ki67+ CD8+ T cells (Fig. 1C and fig. S3). After the first DNA vaccination, the expansion of Ki67+ CD8+ T cells was mainly observed in the vaccine + PD-1 group, although was not significantly different. However, the expansion was prominent in both vaccine groups after the MVA boosts (Fig. 1C). At the peak of MVA vaccinations (i.e., 7 days after each MVA), the frequencies of Ki67+ CD8+ T cells in the vaccine-only and vaccine + PD-1 groups were comparable and were fourfold higher compared with ART-only group (Fig. 1C). The first MVA vaccination also led to a profound increase in the frequency of total CD8+ T cells with cytolytic potential as measured by GrzB and perforin coexpression at week 2 after vaccination (Fig. 1D and fig. S3). While this increase was transient in the vaccine-only group and was not

significantly different compared with control, it persisted in the vaccine + PD-1 group for 14 weeks. After the second MVA boost, the frequency of GrzB and perforin coexpressing CD8+ T cells showed a small expansion in the vaccine + PD-1 but not in the vaccine-only or ART-only animals (Fig. 1D). These results demonstrated that DNA/MVA vaccinations induced high frequencies of proliferating CD8+ T cells with cytolytic potential, and PD-1 blockade markedly enhanced the durability of total CD8+ T cells with cytolytic potential in the blood.

Five weeks after the second MVA boost (1 week before ATI), animals in the vaccine + PD-1 group had significantly higher frequencies of GrzB and perforin coexpressing CD8+ T cells in blood compared with the vaccine-only and ART-only control groups (Fig. 1E). Moreover, we also evaluated the status of FoxP3+ CD4+ and CD8+ T cells [regulatory T cells (Tregs)] in the treated groups. There was no significant difference in the frequency of CD4+ Tregs among three treatment groups. However, animals in the vaccine-only group had marginally higher frequencies of CD8+ Tregs than vaccine + PD-1 and ART-only animals (Fig. 1F and fig. S3). Because the ratio of cytolytic CD8+ T cells and Tregs can influence the function of CD8+ T cells, we measured the ratios (35, 36). The vaccine + PD-1–treated animals exhibited a significantly higher ratio of cells with cytolytic potential to cells with a regulatory phenotype as compared with vaccine-only and ART-only groups (Fig. 1G). This durable and improved cytolytic capability of CD8+ T cells in the vaccine + PD-1–treated animals may be important in controlling HIV/SIV.

DNA/MVA vaccinations induced robust SIV-specific CD4+ and CD8+ T cells with polyfunctionality and breadth in blood

We next investigated the effects of vaccination and PD-1 blockade on SIV-specific T cells response. DNA/MVA vaccinations induced high frequencies of SIV Gag and Env-specific CD4+ and CD8+ T cell cytokine responses (Fig. 2, A and B, and fig. S4A). The frequency of interferon-gamma–positive (IFNλ+) CD4+ and CD8+ T cells increased marginally after two DNA immunizations in both groups (geomean of 0.08% for CD4+ and 0.1% for CD8+), and PD-1 blockade did not enhance these responses. The first MVA strongly boosted both CD4+ and CD8+ IFNλ+ T cell responses with frequencies reaching up to 1% for CD4+ and up to 10% for CD8+ T cells. The boost for CD8+ T cells was comparable for both groups but trended lower for CD4+ T cells in the vaccine + PD-1 group. However, by 5 weeks after first MVA, both CD4+ and CD8+ T cell responses showed better persistence in the vaccine + PD-1 group compared with vaccine-only group (fig. S5, A and B). The SIV-specific IFNλ+ CD4 T cell response contracted ~12-fold (geomean) in vaccine-only group but remained nearly unchanged (fold reduction of ~1) in vaccine + PD-1 group by week 5 after MVA1 (fig. S5A). Similarly, IFNλ+ CD8 T cell response contracted ~5-fold (geomean) in vaccine-only group but remained nearly unchanged (fold reduction of ~1) in vaccine + PD-1 by week 5 after MVA1 boost (fig. S5B). After the second MVA boost, both CD4+ and CD8+ responses were boosted in both groups to a magnitude similar or slightly higher compared with 1 week after MVA1.

In addition to IFNλ, the vaccine-induced T cells also showed an increase in SIV-specific interleukin-2 (IL-2) and tumor necrosis factor–α (TNFα) cytokine responses (fig. S4B)

resulting in the generation of polyfunctional CD4+ and CD8+ T cell responses in both vaccine groups (Fig. 2C and fig. S4, C and D). IFNλ+TNFα+CD8+ T cells were significantly higher only in the vaccine + PD-1 group (fig. S4D). Vaccination also induced significantly higher antigen-specific CD8+ T cell responses in the gut with or without PD-1, resulting in slightly increased polyfunctional CD4+ and CD8+ T cells compared with animals in the ART-only control group (fig. S6, A and B). Vaccination markedly improved SIV antigen recognition breadth of CD4+ and CD8+ T cells (Fig. 2D and fig. S4, E and F). In both of the vaccinated groups, CD4+ T cells recognized an average of 10 to 13 peptide pools, and CD8+ T cells recognized 5 to 6 pools (Fig. 2D). In contrast, the CD4+ and CD8+ T cells in the ART-only control group were generally responsive to less than two pools. Furthermore, vaccinations induced robust SIV Gag-CM9 tetramer–specific CD8+ T cells in Mamu-A* 01+ animals in both groups that ranged from 5 to 17% at day 7 after first MVA and contracted over time (Fig. 2E). The second MVA boost boosted these cells; however, the peak levels were comparable between first and second MVA boosts. At 1 week after the first MVA boost, most of the Gag-CM9 tetramer–positive CD8+ T cells coexpressed GrzB and perforin (Fig. 2F). These results demonstrated that DNA/MVA vaccination during ART induced robust SIV-specific polyfunctional CD4+ and CD8+ T cell responses with strong breadth in blood, with PD-1 blockade enhancing the durability of these responses, at least after the first MVA boost.

DNA/MVA vaccination induced robust CD8+ T cells in the T cell zone and BCFs of the LN

To understand the influence of vaccination on SIV-specific CD4+ and CD8+ T cells in the LNs, we collected LN biopsies at 1 week after the second MVA boost. Phenotypic analysis of the LN CD8+ T cells using flow cytometry revealed higher proliferating CD8+ T cells in the vaccine + PD-1 group, although not significantly different compared with vaccine-only or control groups (Fig. 3A). However, the frequency of GrzB+ perforin+ Ki67+ CD8+ T cells was significantly higher in the vaccine + PD-1 group compared with ART-only group (Fig. 3A). Similarly, the frequency of SIV-specific IFNλ+ CD4+ and CD8+ T cells was also higher in the vaccine + PD-1 group compared with ART-only group (Fig. 3B). The vaccine-only group also showed a marginal increase in the SIV specific IFNλ+ T cell responses but not significantly different compared with control. To gain insight into the localization of SIV-specific CD8+ T cells, we performed in situ GagCM9 tetramer staining of LN sections in Mamu-A*01+ animals in each treatment. GagCM9+ cells were present in both T cell zone (TCZ) and BCF regions of the LN of both vaccine groups (Fig. 3, C and D, and fig. S7, A and B) and expressed GrzB (Fig. 3, C to E, and fig. S7, A and B). The density of these cells was marginally higher in TCZ compared with BCF as previously observed (20) (fig. S7, C and D), and the density of total GagCM9+ T cells correlated positively with the density of total GagCM9+ expressing GrzB (Fig. 3F).

To get a better understanding of the localization of CD8+ T cells in all animals (n = 6 or 7), we investigated the density of bulk cytolytic (GrzB+) CD8+ T cells. Frozen LN sections at MVA2 week 1 time point were stained for CD20 (B cells), CD3 (T cells), CD8, and GrzB (cytolytic protein). We analyzed the magnitude and spatial distribution of CD3+CD8+GrzB+ T cells in the TCZ, BCF, and germinal centers (GCs; Fig. 3, G and H, and fig. S8, A and B). The frequency of CD3+ CD8+GrzB+ T cells was markedly higher in the TCZ and BCF of

vaccinated animals compared with ART-only animals (Fig. 3H). Between the three regions, the density was highest in the TCZ and lowest in GCs (Fig. 3H). While these responses were comparable between the two vaccinated groups, only the vaccine + PD-1 group showed significantly higher CD8+GrzB+ T cells in the GC compartment (Fig. 3H).

Collectively, these data demonstrated that vaccination under ART induced significant localization of the CD8+ T cells having cytolytic potential in the lymphoid tissue compartments, and combining vaccine with anti–PD-1 therapy potentiated their localization in the GCs.

PD-1 blockade potentiated viral reservoir reduction under ART Next, we analyzed cell-associated SIV DNA before vaccination (pre-Vac; 16 weeks after ART) and after vaccination (post-Vac; 5 weeks after second MVA, 1 week before ATI) to understand the influence of vaccination in the absence and presence of PD-1 blockade on viral reservoirs (Fig. 4). Before initiation of ART, the set point viral load (VL) in plasma was relatively higher in the anti– PD-1 group (not significant) compared with ART-only and vaccine-only groups (Fig. 4A). Similarly, at pre-Vac, the DNA reservoir size in the PD-1 group was higher compared with controls (Fig. 4B). To understand this further, we compared the pre-ART set point VL with the pre-Vac reservoir in the LN and observed a trend for positive association, suggesting that the set point VL before initiation of ART contributed to higher reservoir in the vaccine + PD-1 group (Fig. 4C). The lack of significant correlation was primarily due to three animals in the ART-only control group that showed lower reservoir despite having higher set point VL before ART. After vaccination, the reservoir size was comparable between the three groups (Fig. 4D). We analyzed fold difference in the DNA reservoir before and after vaccination and found greater reduction in the vaccine + PD-1 group compared with control and vaccine-only groups together. The vaccine + PD-1 group showed 3.5-fold decline in reservoir compared with 2.1-fold decline in the control and vaccine-only groups (Fig. 4E). These results demonstrated a faster decline of reservoir in the LN of the vaccine + PD-1 group compared with control and vaccine-only group over 9 months and suggested that PD-1 blockade potentiated the reduction of the SIV reservoir. We hypothesized that this was due to the reactivation of the latent cells and/or subsequent clearance of viral antigen–bearing cells by the improved cytolytic CD8+ T cell function in the LNs. This was supported by the positive correlation (Spearman r = 0.8) between fold reservoir reduction and enhanced cytolytic CD8+ T cell density inside the BCF of LN in only the vaccine + PD-1 group after the second MVA (Fig. 4F). To understand the influence of PD-1 blockade plus vaccination on active viral reservoirs, we measured the cell-associated viral RNA before and after vaccination. The magnitude of active reservoir and the fold reduction were not significantly different between the groups (Fig. 4, G to I, and fig. S9, C and D). At pre-Vac, the frequency of viral RNA+, CD4+ cells was nearly 20-fold lower in LN and 24-fold lower in blood compared with viral DNA+ cells, suggesting that the fraction of active viral reservoir was very low under ART (Fig. 4J and fig. S9E). In addition, we did not observe a significant fold reduction for viral DNA reservoir in the blood after vaccination with and without PD-1 blockade (fig. S9B). In summary, we observed a higher decline in the DNA reservoir from pre-Vac to post-Vac in the vaccine + PD-1 group compared with the vaccine-only and ART-only groups.

Combining PD-1 blockade with the vaccination preserved antiviral T cell functions and breadth upon ART interruption

We analyzed SIV-specific responses in the blood starting a week before ATI until 10 weeks after ATI. Before ATI, both vaccine groups showed higher SIV-specific IFNλ+ CD4+ and CD8+ T cell responses compared with ART-only animals (Fig. 5A). After ATI, there was a further expansion of SIV-specific IFNλ+ CD4+ and CD8+ T cells in the vaccine + PD-1 group for 2 to 4 weeks. Similar expansion also occurred in the ART-only group, but there was no significant expansion in the vaccine-only group (Fig. 5A). At 4 weeks after ART, there was no significant difference between the three groups in the blood, although there was a trend for higher IFNλ+ CD4+ and CD8+ T cell magnitude in the vaccine + PD-1 group compared with other two groups (Fig. 5A). In the LN, the IFNλ+ CD8+ T cell response was significantly higher in the vaccine + PD-1 group compared with the ART-only group (Fig. 5B). In addition, SIV-specific CD4+ T cell breadth was marginally higher (trend) in the vaccine + PD-1 group (geomean of ~5 peptide pool recognition) compared with the vaccine-only (geomean of ~3 peptide pool recognition) and ART-only (geomean of ~2 peptide pool recognition) groups (Fig. 5C, top plot). Encouragingly, SIV-specific CD8+ T cell breadth (geomean of ~8 peptide pool recognition) was significantly higher in the vaccine + PD-1 group compared with vaccine-only (geomean of ~3 peptide pool recognition) and ART-only (geomean of ~3 peptide pool recognition) groups (Fig. 5C, bottom plot). A direct comparison of T cell breadth between pre-ATI and post-ATI time points revealed a remarkable preservation of CD8+ T cell breadth in vaccine + PD-1 group but not CD4 T cell (fig. S10, A and B; red). Unexpectedly, the vaccine-only group showed significant loss of T cell breadth after ATI (fig. S10, A and B; blue). The ART-only control animals did not lose T cell breadth or show any significant improvement (fig. S10, A and B; black).

Further analysis of CD8+ T cells in the LN showed the presence of proliferating CD8+ T cells in all groups with a trend toward higher proliferation in the vaccine + PD-1 group (Fig. 5D). However, the proliferation among CXCR5+ was significantly higher in the vaccine + PD-1 group compared with ART-only control group. Further analysis of perforin expression on proliferating CD8+ T cells revealed a significant increase in these cells, both on CXCR5+ and CXCR5− CD8+ T cells, suggesting that PD-1 blockade enhanced the proliferation and cytolytic potential of CD8+ T cells that are expected to be in follicular (CXCR5+) and extrafollicular regions (CXCR5−, TCZ) of LNs. To understand the localization of these CD8+ T cells, we analyzed CD8+GrzB+ T cells in LN sections using immunohistochemistry 4 weeks after ATI. We observed significantly higher localization of CD8+ T cell expressing GrzB in the TCZ and BCF regions of the LN in vaccine + PD-1 group compared with the vaccine-only or ART-only control group (Fig. 5, E and F, and fig. S11, A and B). Unexpectedly, animals in the vaccine-only group did not demonstrate enhanced localization of the GrzB+CD8+ T cells compared with the ART-only group. As expected, the CD8+GrzB+ T cell density was significantly higher in TCZ compared with the BCF overall (fig. S11C). Direct comparison of the CD8+GrzB+T cell densities either within the TCZ or BCF region of the LN section at pre-ATI (after final vaccination) to the post-ATI (week 4) time point revealed notable preservation and significant expansion only in the vaccine + PD-1 upon ART interruption (fig. S11D). The vaccine-only group did not

show any expansion of CD8+GrzB+ T cells. This is consistent with our findings with T cell breadth (fig. S10, A and B). These results demonstrate that PD-1 blockade led to marked preservation of vaccine-induced CD8+ T cell functions after discontinuation of ART.

We next analyzed cytolytic and Tregs in the gut 4 weeks after ATI. Although the frequency of CD8+GrzB+ T cells (Fig. 5G) and CD4+ Tregs (Fig. 5H) was not significantly different between the groups, CD8+ Tregs were significantly lower in vaccine + PD-1 group compared with the other groups (Fig. 5H). Moreover, the vaccine + PD-1 group had a high ratio of GrzB+CD8+ T cells to CD8+ Tregs (Fig. 5I). Collectively, these results showed higher expansion of CD8+ T cells with greater cytolytic potential in blood and TCZ and BCF compartments of LN in vaccine + PD-1 group but not in the vaccine-only group upon discontinuation of ART.

Combining PD-1 blockade with vaccination improved viral control and prolonged survival of the chronically infected monkeys after ATI

We monitored viral rebound in the plasma until 26 weeks after ATI. MVA vaccination was administered in error to two of six animals (RCk16 and RKj16) in the control group 6 weeks before ATI at the time of administration of second MVA to other groups (fig. S12). This resulted in the induction of strong SIV-specific IFNλ+ CD8 T cell response at 1 week after vaccination. In addition, these macaques also showed enhanced proliferation and cytolytic potential (GrzB) of CD8+ T cells after accidental MVA vaccination. Owing to these strong immune responses, we excluded data for these two animals from the control group after MVA2 time point.

After ATI, virus rebounded in all animals by 1 to 3 weeks, and the time to rebound was not considerably different between the groups (Fig. 6A). However, the viral control was significantly better in the vaccine + PD-1 group compared with the ART-only control group up until the study end point (26 weeks after ATI) (Fig. 6, B and C). It is reported that the magnitude of the VL before ART initiation associates with the postrebound viremia (37–39). Therefore, difference in the overall magnitude of the VL between the pre-ART and post-ATI time points should reflect the extent of the viral suppression. We analyzed the difference between the VL area under the curve (AUC) before the ART initiation and after ATI for each animal. This would also account for VL differences over time rather than at a specific time point. After infection, the set point was observed starting week 3 until week 10 at which ART was initiated. Therefore, we calculated pre-ART set point VL AUC from weeks 3 to 10. Similarly, AUC for post-ATI viremia was calculated, and the differences in AUC from pre-ART were analyzed for weeks 3 to 10, 3 to 16, and 3 to 26 (end point) post-rebound (Fig. 6B). The vaccine + PD-1 group showed significantly higher AUC difference compared with the ART-only group at weeks 10, 16, and 24, indicating stronger and persistent suppression of SIV VL after ATI. Consistently, animals in vaccine + PD-1 group but not ART-only and Vaccine-only groups showed significantly lower VLs at week 10, 16, and 26 after ATI compared with the pre-ART VL set point in respective animals (Fig. 6C). We observed a positive correlation between pre-ART VL set point and post-ATI VL set point in ART-only and vaccine- only animals (Fig. 6D and fig. S13; black line). In contrast, we observed a negative association in the vaccine + PD-1 group (fig. S13;

red line). These data suggested that the addition of PD-1 blockade to vaccination altered the immune response, allowing for better viral control after ART interruption compared with ART-only and vaccine-only groups, and this improvement was better in animals with higher set point VL.

Animals in the vaccine + PD-1 group had a significant delay in their time to reach pre-ART set point VL (Fig. 6E). Four of the six RMs in the vaccine-only group and all of the ART-only group RMs reached pre-ART set point by the study end point (26 weeks). In contrast, only one of seven RMs in the vaccine + PD-1 group reached their pre-ART set point by this time point. The macaque in this group that reached its pre-ART set point (ID 9Q7) showed poor SIV-specific T cell response and breadth upon vaccination and subsequently died due to non-AIDS–related reasons that were not related to any treatment interventions (fig. S14, A and B). Consistent with their better viral control, animals in the vaccine + PD-1 group had significantly improved survival compared with the vaccine-only and ART-only control group (Fig. 6F). None of the RMs in the vaccine + PD-1 group progressed to AIDS as opposed to 50% of the animals in the ART-only and vaccine-only groups (Fig. 6F and table S1). The vaccine-only group had significantly higher CD4+ T cell activation in comparison to the ART-only and vaccine + PD-1 groups (Fig. 6G). CD4+ T cell frequencies in gut were not significantly different between the groups (fig. S15A), although the vaccine + PD-1 group showed marginally higher frequency at week 10 (fig. S15B) and week 16 (fig. S15C) after ATI. We also observed lower immune activation of CD4+ T cells in the gut of vaccine + PD-1 group animals as measured by lower Ki67+HLA-DR+CD4+ T cells (Fig. 6H). In addition, the vaccine + PD-1 group demonstrated lower neutrophil frequency and higher lymphocyte and CD8 T cell counts pointing to lower inflammatory condition and better immune reconstitution compared with ART-only control and vaccine-only groups (fig. S16). Together, these findings show enhanced viral control, improved health, and survival benefits in vaccine + PD-1–treated animals. We additionally analyzed a blood clinical chemistry profile that includes various proteins, ions, enzymes, and glucose to account for any adverse effects of the interventions and observed no significant changes in these biochemical parameters, indicating that the therapy was safe (fig. S17).

Correlation analyses with the AUC differences (viral control) of VL set point between pre-ART (weeks 3 to 10) and post-ATI (weeks 3 to 10) revealed various correlates. Fold reduction in SIV DNA reservoir in LN but not in blood showed significant positive correlation with the AUC difference (Fig. 6I and fig. S8F). Several CD8 T cell properties correlated positively with the viral control (Fig. 6J). Proliferating Ki67+CD8+ T cells having BCF-homing potential (CXCR5+) expressing one or more cytolytic markers in the LN after ATI showed significant positive correlation with the enhanced viral control (Fig. 6J). Similarly, antigen-specific IFNλ+CD8+ T cells within LNs correlated positively with the SIV control. Together, these results suggest that highly functional SIV-specific CD8+ T cells demonstrated that vaccination with CD40L and TLR7 agonist– adjuvanted DNA/MVA vaccination under ART induced robust and broad SIV-specific CD4+ and CD8+ T cell responses with a polyfunctional profile and cytolytic potential in blood and LNs. Vaccination also generated a strong SIV-specific CD8+ T cell response with cytolytic potential in TCZ and BCF regions of LN, much needed immune component to achieve a cure against HIV. Administration of PD-1 blockade during vaccination did not further

improve the magnitude and breadth of vaccine-induced T cell response in blood but improved the cytolytic potential of CD8+ T cells. In the LN, the frequency of SIV-specific CD8+ T cells and the density of GrzB+ CD8+ cells in the GC were higher only in the PD-1–treated group but not in the vaccine-only group compared with control group. This was associated with greater reduction in LN viral reservoirs in the PD-1–treated group. After ATI, the viral control and survival were better in the PD-1–treated group, and these were associated with better preservation of breadth of CD8+ T cell in the LN combined with reservoir reduction are key in controlling viremia after ATI.

DISCUSSION

A successful HIV cure is limited by inefficient elimination of persistent viral reservoirs, restricted homing of cytotoxic CD8+ T cells into the BCF, a known viral reservoir sanctuary, and diminished CD4+ and CD8+ T cell functions despite effective ART therapy. Current strategies fail to efficiently combine LRAs with the induction and homing of functional HIV/SIV-specific cellular immunity to viral reservoir sites in LNs. Immune checkpoint blockade alone fails to purge latent reservoirs or control rebounding viremia in a chronic SIV/macaque infection model (34), highlighting the need for combining immune checkpoint blockade with the other interventions such as vaccination and passive antibody therapy. The results from our study demonstrated that vaccination with CD40L and TLR7 agonist–adjuvanted DNA/MVA vaccination under ART induced robust and broad SIV-specific CD4+ and CD8+ T cell responses with a polyfunctional profile and cytolytic potential in blood and LNs. Vaccination also generated a strong SIV-specific CD8+ T cell response with cytolytic potential in TCZ and BCF regions of LN, much needed immune component to achieve a cure against HIV. Administration of PD-1 blockade during vaccination did not further improve the magnitude and breadth of vaccine-induced T cell response in blood but improved the cytolytic potential of CD8+ T cells. In the LN, the frequency of SIV-specific CD8+ T cells and the density of GrzB+ CD8+ cells in the GC were higher only in the PD-1–treated group but not in the vaccine-only group compared with control group. This was associated with greater reduction in LN viral reservoirs in the PD-1–treated group. After ATI, the viral control and survival were better in the PD-1–treated group, and these were associated with better preservation of breadth of CD8+ T cell response in blood and the presence of higher density of CD8+ T cells in the TCZ and BCF with cytolytic potential in the LN. In summary, these results demonstrated that the combination of PD-1 blockade and therapeutic vaccination can be used to generate a highly functional and broad SIV-specific CD8+ T cell response in blood and LNs that can be sustained after ATI. They also highlight a potential therapeutic approach that may help achieve a cure to HIV.

Although the viral control we observed in the vaccine + PD-1 group compared with control was not profound, we think even a fivefold effect is meaningful for the following reasons. The chronic infection model (SIVmac239/RM) used in this study sets a very high barrier to cure because SIVmac239 establishes set point VL in the order of 106 copies/ml, which is about 100 times greater compared with the set point VL established by HIV-1 in humans. Consistently, SIVmac infection in RMs seed a significantly higher proportion of reservoirs compared with HIV-1 in humans (40). The high set point VL combined with initiation of ART at 10 weeks after infection also leads to the establishment of a

high SIV reservoir, immune dysfunction, and viral escape from antiviral immunity. Recent studies using the same virus and model fail to show any effect on viral control or reservoir despite showing clear latency reversal effect of immune checkpoint blockade (34, 41). Therefore, it is encouraging that our current study achieved moderate but persistent viral control with no AIDS progression using the highly stringent SIVmac239 RM model of HIV/AIDS. Nevertheless, these results highlighted that curing HIV/SIV infection necessitates resolving these multilayered limitations. In this direction, initiating ART early after infection may result in more marked viral control after ART interruption because of less reservoir seeding and less escape variants. Consistently, starting ART 9 days after infection results in lower reservoir seeding and better viral control (42). Therefore, combining early ART with vaccination and PD-1 blockade may result in stronger viral control in the absence of ART.

Several CD8+ T cell functions correlated with viral control. The primary correlate in our study was the induction and maintenance of highly functional and broad CD8+ T cell response with the ability to home to BCF (CXCR5+GrzB+ and perforin+ CD8+ T cells), where most of the SIV reservoirs persist. Consistently, we observed greater reservoir reduction in the vaccine + PD-1 group. These results highlighted the importance of inducing cytotoxic CD8 T cells that can home to lymphoid tissue. Furthermore, combining the vaccine with PD-1 blockade resulted in striking durability of CD8+ T cell function in the blood, LN, and gut compared with vaccine-only animals after ATI. We also found that PD-1 blockade more consistently improved the proliferation and cytolytic potential of SIV-specific CD8+ T cells in the LN compared with the vaccine-only animals as indicated by a higher proliferation of CXCR5+GrzB+ and perforin+ CD8+ T cells and follicular homing. It is worth noting that the PD-1 blockade in an LCMV model associates with the proliferative burst of a specific CXCR5+ Tcf-1+ CD8+ T cell population, which shows stem cell–like properties (43). This population predominantly resides in the TCZ but not in the BCFs. While several studies, including ours, show the association of the ability of CXCR5+ CD8+ T cells to translocate into BCF with better viral control (20, 44–46), it remains to be established whether this population is exclusively coming from Tcf-1+ stem cell– like CXCR5+ CD8+ T cells residing in TCZ during HIV infection and whether these cells also require CXCR5+ expression to home to BCF.

We do not know the specificity of GrzB+ and perforin+ CD8+ T cells that were increased in the LNs upon vaccination with or without PD-1 blockade. Frequency of these cells was much larger than what we scored in antigen-specific cytokine response assay. Unfortunately, we could not combine staining for the cytolytic molecules and cytokines in our intracellular cytokine assays because cells rapidly degranulate and lose intracellular cytolytic molecules immediately after stimulation. We also do not know whether these CD8+ T cells in the LNs expressing cytolytic marker were able to kill the virus-infected cells. Previous studies in chronically HIV-infected humans and SIV-infected RMs report compromised cytolytic activity of HIV/SIV-specific CD8+ T cells in LNs (19, 47). Furthermore, most of the virus-specific CD8+ T cells are excluded from the BCF in the chronic HIV/SIV infection setting (18, 48, 49). At present, several strategies are being tested to facilitate homing of antigen-specific CD8+ T cells with cytolytic potential into the BCF and killing of infected cells (50–52). Here, we have shown that vaccination induced robust CD8+ T cells having cytolytic potential into the LNs. However, further investigations are needed to establish

whether these cells are capable of directly killing infected cells and reducing the viral reservoirs in GC–follicular helper T cells located in BCF.

Animals in the vaccine-only group failed to show sustained SIV-specific CD8+ T cell response and functions after ATI despite inducing a strong and highly functional T cell response after vaccination. The precise mechanisms behind the loss of T cell breadth and localization to BCF after ATI remain to be determined. Hyperimmune activation and disease progression correlate with sustained elevation of type I IFN responses in SIV-infected RMs (53–55), and previous reports show that sustained type I IFNs during chronic HIV infection impair CD8+ T cell function and survival, and blocking IFN receptor can rescue these immune defects (56). PD-1 blockade potently down-regulates interferon stimulated genes (ISGs) (23, 57), and this ISG down-regulation persists long after discontinuation of anti–PD-1 antibody therapy (57). Here, we observed significantly lower frequency of neutrophil and significantly higher CD8+ T cell count in vaccine + PD-1 group, at week 10 after ART interruption, compared with control. Therefore, it is likely that PD-1 blockade in the vaccine + PD-1 group mediated dampening of chronic inflammation, and this could have contributed to better and sustained functional quality of CD8+ T cells after ATI.

The timing of PD-1 blockade is critical because PD-1 blockade not only reverses CD8+ T cell exhaustion but also can reverse latency. Therefore, we considered using PD-1 blockade primarily at three time points, i.e., before initiation of ART (phase 1), during vaccination under ART (phase 2), and after ATI (phase 3). As indicated above and observed in our previous study (23), the goal for phase 1 was to restore CD8+ T cell function that may lead to faster viral pull down and seeding of lower viral reservoirs. However, in this study, we did not observe restoration of CD8+ T cell function and faster pull down of virus after ART initiation. We think that this could be due to some important differences between the two studies such as the use of vaccinated monkeys in the prior study, prolonged chronic infection (24 to 30 weeks versus 10 weeks) before ART initiation, and virus variants used for infection (SIVmac251 versus SIVmac239). Nevertheless, we cannot rule out whether PD-1 blockade during phase 1 influenced some of the intrinsic T cell functions that we have not characterized. The PD-1 blockade under ART (phase 2) showed clear therapeutic benefits by potentiating reservoir reduction and inducing strong antiviral response in the LNs. However, we did not use the PD-1 blockade following ATI (phase 3) because the animals developed strong antidrug antibody response. However, we believe that viral control can be further improved by PD-1 blockade after ART interruption because we and others observed greater viral control when PD-1 was given after ART interruption (58, 59). Moreover, a PD-1 alone arm was absent in the current study, which would have facilitated a better understanding of the effect of vaccine + PD-1 combination compared with PD-1 alone. More studies are needed to clearly establish the most optimal timing for PD-1 blockade in reaping the maximum therapeutic benefits. Moreover, a PD-1 alone arm was absent in the current study, which would have facilitated a better understanding of the effect of vaccine + PD-1 combination compared with PD-1 alone.

In conclusion, this study using the SIV/macaque model assessed the potential of combining therapeutic vaccination and PD-1 immune checkpoint blockade toward the ultimate goal of achieving HIV cure in the chronic infection setting. The therapeutic potential of vaccine +

PD-1 blockade might be improved by combining it with other immune checkpoint blockade approaches, such as PD-1 and cytotoxic T-lymphocyte-associated protein-4 (CTLA-4) dual blockade, LRAs, such as AZD5582, and anti-inflammatory agents, such as IL-10 and IFNR blockade. However, combining multiple therapeutic approaches could also increase the safety concerns. At present, several clinical trials are underway or have finished testing PD-1 blockade therapy alone or in combination with other immune checkpoint blockade agents in different HIV-1 infection settings (60–64). It is currently unknown, however, whether these therapies will be safe and tolerable in HIV-infected individuals. Nevertheless, our findings carry potential implications for the development of an effective therapy for HIV/AIDS.

MATERIALS AND METHODS

Study design

The objective of this study was to test the therapeutic benefits of combining PD-1 blockade and vaccination against HIV/AIDS using a chronic SIV/macaque model. We used a DNA/MVA vaccination regimen to induce strong, broad, and durable antiviral CD8+ T cell immunity under ART and combined it with PD-1 blockade that can further improve CD8+ T cell functional quality, reduce viral reservoir, and thereby control viral rebound upon ART discontinuation. To achieve this, we infected three groups of RMs with SIVmac239 intrarectally to induce chronic infection and initiated ART at 10 weeks after infection. Two groups were subsequently immunized with a CD40L plus TLR7 agonist–adjuvanted DNA/MVA SIV239 vaccine alone (vaccine-only, n = 6) or in combination with anti–PD-1 antibody therapy (vaccine + PD-1, n = 7). The third group did not receive vaccination or anti–PD-1 antibody therapy and served as the ART-only control group (control, n = 6). All vaccinations were carried out under complete viral suppression by ART. ATI was done at week 66 (6 weeks after the second MVA boost), and RMs were followed for 26 weeks after ATI to check for viral rebound, development of AIDS, and survival.

Vaccines and immunizations

The construction of CD40L-adjuvated DNA (65) and MVA (66) vaccines has been described previously. The DNA vaccine expressed SIV239 Gag-Pol, Env, Tat, and Rev, and macaque CD40L. Two milligrams of DNA vaccine was reconstituted in 666 μl of phosphate-buffered saline (PBS). The total dose was injected over six sites each with 100 μl per dose. Immediately after intradermal DNA administration, a needle array electrode (6-needle, 4-mm length and 2-mm depth; procured from BTX) was placed over the raised skin area (bleb) of injection, and voltage was applied (two pulses, 1125 V/cm, 50 μs + 8 pulses, 275 V/cm, 10 ms). MVA-SIVgpe or DR1 was a gift by B. Moss and expressed SIVmac239 Gag, PR, RT, and Env. A total of 1-ml of MVA containing 108 plaque-forming units per dose was divided into two 0.5-ml injections given IM into each quadricep. Young adult Indian RMs from the Yerkes breeding colony were selected on the basis of Mamu-A*01, Mamu-B*08, and Mamu-B*17 alleles as shown in table S1. The Animal Welfare Act and National Institutes of Health (NIH) (Bethesda, MD) Guide for the Care and Use of Laboratory Animals were followed. Protocols were approved by the Emory University Institutional Animal Care and Use Committee. The monkey infectious dose 50 for intrarectal challenge was calculated to be 1150 median tissure culture infectious dose (TCID50). All

RMs were infected intrarectally with 1000 to 3000 TCID50 of SIVmac239, and ART was initiated at 9.4 weeks. ART regimen consisted of three ART drugs emtricitabine (40 mg/kg), tenofovir disoproxil fumarate (5.1 mg/kg), and dolutegravir (2.5 mg/kg) and was administered subcutaneously. ATI was done at week 66 after infection, and macaques were followed for 26 weeks after ATI for VL and until 36 weeks for survival. The progression of AIDS was determined on the basis of the following parameters: weight loss, recurrent diarrhea, loss of appetite, and thrombocytopenia. The decision on when to euthanize an animal was made by veterinarians who were blinded to study groups.

Imiquimod treatment—Imiquimod was purchased as a topical cream (5% imiquimod; Aldara) and was applied topically on the dorsal skin of the monkeys near shoulder girdle. It was applied at 6 and 24 hours after each DNA vaccination at the site of injection. In addition, four ectopic applications were given every 2 weeks after the first MVA boost and two applications every 2 weeks after the second MVA boost.

Anti–PD-1 antibody treatment—The anti–PD-1 antibody (clone EH12) was primatized as described previously (23). Each macaque received PD-1 blockade in two phases: phase 1 with five doses on days 0, 3, 7, 10, and 14 at 3 mg/kg starting 10 days before the initiation of ART as done previously (23). In the phase 2, three doses of 10 mg/kg were given at weeks 38, 41, and 44 concomitant with the DNA priming.

Antibodies

Antibodies used in this study are as follows: CD3 (clone SP-34–2; BD Biosciences), CXCR5 (MU5UBEE; eBioscience), GagCM9 tetramer (NIH tetramer core), CD28 (CD28.2; eBioscience), CD95 (DX2; BD Biosciences), CD279 (PD-1; clone EH12.2H7; BioLegend), CD8 (SK1; BD Bioscience), Ki67 (B56; BD Biosciences), CD4 (L200; BD Biosciences), GrzB (GB11; BD Biosciences), perforin (Pf-344; Mabtech), FoxP3 (206D; BioLegend), HLA-DR (L243; BioLegend), IFNλ (B27; BD Biosciences), TNFα (MAb11; BD Biosciences), and IL-2 (MQ1- 17H12; BD Biosciences).

Phenotyping and intracellular cytokine staining

Phenotyping—Mononuclear cells were isolated from rectum and axillary LNs as described previously (20, 21, 23). Whole blood and mononuclear cells from tissues were stained with LIVE/DEAD Near-IR Dead Cell stain (Life Technologies) and antibodies specific to CD3, CD4, CD8, PD-1, HLA-DR, Gag-CM9, CD28, and CD95. To stain cells with intracellular markers, cells were fixed and permeabilized with the eBioscience FoxP3/ Transcription Factor staining buffer set following the manufacturer's instructions and stained with antibodies specific to FoxP3, Ki67, GrzB, and perforin. These samples were acquired on an LSR Fortessa (BD Biosciences).

Intracellular cytokine staining—Mononuclear cells were processed from blood, gut, and axillary LNs, and intracellular cytokine staining (ICCS) assays were performed as previously described (21, 23). Cells were stimulated using peptide pools spanning the entire SIV-Env protein [peptide (2 μg/ml); single pool of 218 peptides; catalog no. 12635; NIH AIDS Research and Reagent Program] and SIV-Gag protein [peptide (4 μg/ml); single

pool of 125 peptides; catalog no. 12364; NIH AIDS Research and Reagent Program]. Stimulation with phorbol 12-myristate 13-acetate (80 ng/ml) and ionomycin (1 μg/ml) and unstimulated samples served as positive and negative controls. Cells were stimulated for 2 hours, Golgistop and GolgiPlug were added, and stimulated for an additional 4 hours. For mapping SIV-specific T cell breadth, 125 individual (SIV)mac239 Gag peptides (catalog no. 6204; NIH AIDS Research Reagent) were pooled into 12 minipools with ~10 peptides per pool. Similarly, 218 individual (SIV)mac239 Env peptides (catalog no. 6883; NIH AIDS Research Reagent) were pooled into 12 minipools having ~18 peptides per pool.

Enzyme-linked immunosorbent assay for ADA response

To measure the ADA response generated against the infused primatized EH12 monoclonal antibody (mAb), plates were coated with the primatized EH12 mAb (2.5 μg/ml) in PBS overnight. Dilutions (1:50, 1:100, and 1:150) of plasma samples were incubated before the addition of mouse anti-monkey immunoglobulin G1 (IgG1)–Biotin (SB108a, SouthernBiotech) to detect bound antibody. One hundred microliters of horseradish peroxidase–streptavidin was added at a dilution of 1:1000, and 3,3’,5,5’-tetramethylbenzidine (TMB) peroxidase substrate Kirkegaard and Perry Labs (KPL) was used for development. The reaction was stopped with 1 N H3PO4, and absorbance was read at 450 nm.

Immunohistochemistry and confocal microscopy

Tissue imaging of optimum cutting temperature (OCT) compound– embedded tissue sections was performed as described previously (20). Briefly, freshly harvested LNs from SIVmac239-infected macaques were fixed in 4% paraformaldehyde (PFA) for 30 min at room temperature followed by embedding in OCT compound and freezing. Ten- to 20-μm-thick tissue sections were taken from frozen OCT blocks and adhered to highly adhesive glass slides. Tissue sections were blocked with 5% bovine serum albumin (BSA) in PBS supplemented with 2% donkey serum and 0.025% Triton X-100 for 1 hour at room temperature. After three washes with chilled PBS, tissue sections were incubated overnight with primary antibodies in 1% BSA and 0.025% Triton X-100 supplemented PBS. For investigating cytolytic CD8+ T cells inside BCFs, the primary antibody cocktail contained rabbit anti-hCD8 (Invitrogen, catalog no. MA1-81692), mouse GrzB (clone GB11, Invitrogen, catalog no. MA1-80734), and goat anti-hCD20 (LSBio, LS-B11144). The next day, the primary antibodies were washed off the slides three times using chilled PBS followed by incubation with secondary antibodies for 1 hour at room temperature. The secondary antibody cocktail contained anti-rabbit IgG–Alexa 488 (Invitrogen, catalog no. A21206), anti-mouse IgG– Alexa 555 (Invitrogen, catalog no. A31570), and anti–goat–Alexa 405 (Abcam, catalog no. ab175664). Slides were washed three times with chilled PBS and mounted using anti-fade mounting media followed by confocal imaging. Imaging was performed on Olympus FV1000 using 20Å~ objective, and images were analyzed using ImageJ and QuPath using automated cell detection plugin.

In situ tetramer staining combined with immunohistochemistry

In situ tetramer staining combined with immunofluorescent staining was performed as previously described (20). Briefly, about 1- to 2-mm-thick sections of tissue were excised

manually using fresh LN by a surgical scalpel. Sections were incubated with 0.5 to 1μg of fluorescein isothiocyanate (FITC)–labeled tetramer loaded with SIV Gag CM9 (181 to 189) (CTPYDINQM) peptide for 16 to 24 hours at 4ÅãC. Tetramer-treated sections were washed three times (20 min per wash) with chilled PBS followed by fixation with 2% PFA at 4ÅãC for 20 min. Next, fixed sections were washed with chilled PBS and incubated with primary antibodies. Two sets of staining were performed— the first panel had CD3, GagCM9 tetramer, and CD20 combination, and the other panel had CD8, GagCM9-tetramer, GrzB, and CD20 combinations. The primary antibodies for the first panel included rabbit anti-FITC (AbDSerotec), rat anti-hCD3 (Bio-Rad, catalog no. mca1477), and mouse anti hCD20 (NCL-L-CD20, L26). The primary antibodies for second panel included rabbit anti-FITC (AbDSerotec), rat anti-hCD8 (Invitrogen, catalog no. MA1-81692), and mouse anti-GrzB (clone GB11, Invitrogen, catalog no. MA1- 80734). After overnight incubation with primary antibodies, sections were washed thrice with PBS as mentioned before followed by a 2-hour incubation with corresponding secondary/tertiary antibodies. For the first panel, the secondary antibody cocktail constituted of anti-rabbit IgG–Alexa 488 (Jackson ImmunoResearch), anti-mouse IgG–Alexa 555 (Molecular Probes), anti-rat IgG-Cy5 (Jackson ImmunoResearch). For the second panel, the secondary antibody cocktail constituted of anti-rat IgG–Alexa 647, anti-mouse IgG–Alexa 555, anti-rabbit IgG–Alexa 488, and direct PacBlue conjugate against CD20. Slides were washed thrice with chilled PBS and mounted using anti-fade mounting media followed by confocal imaging. Imaging was performed on Olympus FV1000 using 20Å~ objective, and images were analyzed using ImageJ software and QuPath automated cell detection plugin.

Cell-associated DNA and RNA quantification

Cell-associated SIV-DNA and RNA were simultaneously measured in sorted CD4+ T cells from LN and blood as previously described (41). CD4+ T cells were sorted using a nonhuman primate CD4+ isolation kit (Miltenyi, catalog no. 130-092-144) as per the manufacturer’s protocol.

Statistical analyses

All graphs, significance, and correlations were analyzed using GraphPad Prism (v8). P values were calculated using Mann Whitney U or Wilcoxon test. Correlations were analyzed using nonparametric Spearman correlation and Pearson wherever indicated. Bonferroni correction was performed for multiple comparisons wherever applicable. $P \leq 0.05$ was considered significant.

Supplementary Material

Refer to Web version on PubMed Central for supplementary material.

Acknowledgments:

We thank S. Ehnert, J. Sherrie, and all the veterinary staff at Yerkes for animal care; L. Shan and CFAR virology core for viral RNA and CA SIV DNA analysis; and K. Gill, B. Cervasi, and CFAR immunology core for help with flow cytometry. The SIVmac239 strain used to infect the RMs was provided by G. Silvestri at Emory University School of Medicine, and anti-Gag tetramers were provided by NIH Tetramer Core Facility at Emory. We thank R.

Wang and K. Reimann at the University of Massachusetts Medical School for the RM constant regions of the IgG4 used in EH12 (anti-PD-1) mAb. We thank V. Velu for constructive discussion.

Funding:

This work was supported by the NIH R37AI112787 to R.R.A., P01AI056299 to G.J.F., NCRR/NIH base grant P51 OD011132 to Yerkes National Primate Research Center; and Emory CFAR grant P30 AI050409. S.A.R. and B.Y. are the recipients of AIDS Vaccine 200 fellowship award. This research project was supported in part by the Emory University Integrated Cellular Imaging Microscopy Core.

Data and materials availability:

All data needed to evaluate the conclusions in the paper are present in the paper or the Supplementary Materials.

REFERENCES AND NOTES

1. Cockerham LR, Jain V, Sinclair E, Glidden DV, Hartogenesis W, Hatano H, Hunt PW, Martin JN, Pilcher CD, Sekaly R, McCune JM, Hecht FM, Deeks SG, Programmed death-1 expression on CD4+ and CD8+ T cells in treated and untreated HIV disease. AIDS 28, 1749–1758 (2014). [PubMed: 24871455]
2. Day CL, Kaufmann DE, Kiepiela P, Brown JA, Moodley ES, Reddy S, Mackey EW, Miller JD, Leslie AJ, Depierres C, Mncube Z, Duraiswamy J, Zhu B, Eichbaum Q, Altfeld M, Wherry EJ, Coovadia HM, Goulder PJ, Klenerman P, Ahmed R, Freeman GJ, Walker BD, PD-1 expression on HIV-specific T cells is associated with T-cell exhaustion and disease progression. Nature 443, 350–354 (2006). [PubMed: 16921384]
3. Paiardini M, Muller-Trutwin M, HIV-associated chronic immune activation. Immunol. Rev 254, 78–101 (2013). [PubMed: 23772616]
4. Plaeger SF, Collins BS, Musib R, Deeks SG, Read S, Embry A, Immune activation in the pathogenesis of treated chronic HIV disease: A workshop summary. AIDS Res. Hum. Retroviruses 28, 469–477 (2012). [PubMed: 21854232]
5. Rajasuriar R, Khoury G, Kamarulzaman A, French MA, Cameron PU, Lewin SR, Persistent immune activation in chronic HIV infection: Do any interventions work? AIDS 27, 1199–1208 (2013). [PubMed: 23324661]
6. Chomont N, El-Far M, Ancuta P, Trautmann L, Procopio FA, Yassine-Diab B, Boucher G, Boulassel MR, Ghattas G, Brenchley JM, Schacker TW, Hill BJ, Douek DC, Routy JP, Haddad EK, Sekaly RP, HIV reservoir size and persistence are driven by T cell survival and homeostatic proliferation. Nat. Med 15, 893–900 (2009). [PubMed: 19543283]
7. Colby DJ, Trautmann L, Pinyakorn S, Leyre L, Pagliuzza A, Kroon E, Rolland M, Takata H, Buranapraditkun S, Intasan J, Chomchey N, Muir R, Haddad EK, Tovanabutra S, Ubolyam S, Bolton DL, Fullmer BA, Gorelick RJ, Fox L, Crowell TA, Trichavaroj R, O'Connell R, Chomont N, Kim JH, Michael NL, Robb ML, Phanuphak N, Ananworanich J; The RV411 study group, Rapid HIV RNA rebound after antiretroviral treatment interruption in persons durably suppressed in Fiebig I acute HIV infection. Nat. Med 24, 923–926 (2018). [PubMed: 29892063]
8. Deleage C, Wietgrefe SW, Del Prete G, Morcock DR, Hao XP, Piatak M Jr., Bess J, Anderson JL, Perkey KE, Reilly C, McCune JM, Haase AT, Lifson JD, Schacker TW, Estes JD, Defining HIV and SIV Reservoirs in Lymphoid Tissues. Pathog. Immun 1, 68–106 (2016). [PubMed: 27430032]
9. Murray AJ, Kwon KJ, Farber DL, Siliciano RF, The latent reservoir for HIV-1: How immunologic memory and clonal expansion contribute to HIV-1 persistence. J. Immunol 197, 407–417 (2016). [PubMed: 27382129]
10. Whitney JB, Hill AL, Sanisetty S, Penaloza-MacMaster P, Liu J, Shetty M, Parenteau L, Cabral C, Shields J, Blackmore S, Smith JY, Brinkman AL, Peter LE, Mathew SI, Smith KM, Borducchi EN, Rosenbloom DI, Lewis MG, Hattersley J, Li B, Hesselgesser J, Geleziunas R, Robb ML, Kim JH, Michael NL, Barouch DH, Rapid seeding of the viral reservoir prior to SIV viraemia in rhesus monkeys. Nature 512, 74–77 (2014). [PubMed: 25042999]

11. Zajac AJ, Blattman JN, Murali-Krishna K, Sourdive DJ, Suresh M, Altman JD, Ahmed R, Viral immune evasion due to persistence of activated T cells without effector function. J. Exp. Med 188, 2205–2213 (1998). [PubMed: 9858507]
12. Zicari S, Sessa L, Cotugno N, Ruggiero A, Morrocchi E, Concato C, Rocca S, Zangari P, Manno EC, Palma P, Immune activation, inflammation, and non-AIDS co-morbidities in HIV-infected patients under long-term ART. Viruses 11, 200 (2019).
13. Banga R, Procopio FA, Noto A, Pollakis G, Cavassini M, Ohmiti K, Corpataux JM, de Leval L, Pantaleo G, Perreau M, PD-1+ and follicular helper T cells are responsible for persistent HIV-1 transcription in treated aviremic individuals. Nat. Med 22, 754–761 (2016). [PubMed: 27239760]
14. Fromentin R, Bakeman W, Lawani MB, Khoury G, Hartogensis W, DaFonseca S, Killian M, Epling L, Hoh R, Sinclair E, Hecht FM, Bacchetti P, Deeks SG, Lewin SR, Sekaly RP, Chomont N, CD4+ T cells expressing PD-1, TIGIT and LAG-3 contribute to HIV persistence during ART. PLOS Pathog. 12, e1005761 (2016). [PubMed: 27415008]
15. Fukazawa Y, Lum R, Okoye AA, Park H, Matsuda K, Bae JY, Hagen SI, Shoemaker R, Deleage C, Lucero C, Morcock D, Swanson T, Legasse AW, Axthelm MK, Hesselgesser J, Geleziunas R, Hirsch VM, Edlefsen PT, Piatak M Jr., Estes JD, Lifson JD, Picker LJ, B cell follicle sanctuary permits persistent productive simian immunodeficiency virus infection in elite controllers. Nat. Med 21, 132–139 (2015). [PubMed: 25599132]
16. McGary CS, Deleage C, Harper J, Micci L, Ribeiro SP, Paganini S, Kuri-Cervantes L, Benne C, Ryan ES, Balderas R, Jean S, Easley K, Marconi V, Silvestri G, Estes JD, Sekaly RP, Paiardini M, CTLA-4+PD-1− memory CD4+ T cells critically contribute to viral persistence in antiretroviral therapy-suppressed, SIV-infected rhesus macaques. Immunity 47, 776–788.e5 (2017). [PubMed: 29045906]
17. Shen A, Zink MC, Mankowski JL, Chadwick K, Margolick JB, Carruth LM, Li M, Clements JE, Siliciano RF, Resting CD4+ T lymphocytes but not thymocytes provide a latent viral reservoir in a simian immunodeficiency virus-Macaca nemestrina model of human immunodeficiency virus type 1-infected patients on highly active antiretroviral therapy. J. Virol 77, 4938–4949 (2003). [PubMed: 12663799]
18. Li S, Folkvord JM, Kovacs KJ, Wagstaff RK, Mwakalundwa G, Rendahl AK, Rakasz EG, Connick E, Skinner PJ, Low levels of SIV-specific CD8+ T cells in germinal centers characterizes acute SIV infection. PLOS Pathog. 15, e1007311 (2019). [PubMed: 30897187]
19. Reuter MA, Del Rio Estrada PM, Buggert M, Petrovas C, Ferrando-Martinez S, Nguyen S, Sada Japp A, Ablanedo-Terrazas Y, Rivero-Arrieta A, Kuri-Cervantes L, Gunzelman HM, Gostick E, Price DA, Koup RA, Naji A, Canaday DH, Reyes-Teran G, Betts MR, HIV-specific CD8+ T cells exhibit reduced and differentially regulated cytolytic activity in lymphoid tissue. Cell Rep. 21, 3458–3470 (2017). [PubMed: 29262326]
20. Mylvaganam GH, Rios D, Abdelaal HM, Iyer S, Tharp G, Mavinger M, Hicks S, Chahroudi A, Ahmed R, Bosinger SE, Williams IR, Skinner PJ, Velu V, Amara RR, Dynamics of SIV-specific CXCR5+ CD8 T cells during chronic SIV infection. Proc. Natl. Acad. Sci. U.S.A 114, 1976–1981 (2017). [PubMed: 28159893]
21. Velu V, Titanji K, Zhu B, Husain S, Pladevega A, Lai L, Vanderford TH, Chennareddi L, Silvestri G, Freeman GJ, Ahmed R, Amara RR, Enhancing SIV-specific immunity in vivo by PD-1 blockade. Nature 458, 206–210 (2009). [PubMed: 19078956]
22. Finnefrock AC, Tang A, Li F, Freed DC, Feng M, Cox KS, Sykes KJ, Guare JP, Miller MD, Olsen DB, Hazuda DJ, Shiver JW, Casimiro DR, Fu TM, PD-1 blockade in rhesus macaques: Impact on chronic infection and prophylactic vaccination. J. Immunol 182, 980–987 (2009). [PubMed: 19124741]
23. Mylvaganam GH, Chea LS, Tharp GK, Hicks S, Velu V, Iyer SS, Deleage C, Estes JD, Bosinger SE, Freeman GJ, Ahmed R, Amara RR, Combination anti–PD-1 and antiretroviral therapy provides therapeutic benefit against SIV. JCI Insight 3, e122940 (2018).
24. Hammerich L, Marron TU, Upadhyay R, Svensson-Arvelund J, Dhainaut M, Hussein S, Zhan Y, Ostrowski D, Yellin M, Marsh H, Salazar AM, Rahman AH, Brown BD, Merad M, Brody JD, Systemic clinical tumor regressions and potentiation of PD1 blockade with in situ vaccination. Nat. Med 25, 814–824 (2019). [PubMed: 30962585]

25. Mougel A, Terme M, Tanchot C, Therapeutic cancer vaccine and combinations with antiangiogenic therapies and immune checkpoint blockade. Front. Immunol 10, 467 (2019). [PubMed: 30923527]
26. Soares KC, Rucki AA, Wu AA, Olino K, Xiao Q, Chai Y, Wamwea A, Bigelow E, Lutz E, Liu L, Yao S, Anders RA, Laheru D, Wolfgang CL, Edil BH, Schulick RD, Jaffee EM, Zheng L, PD-1/PD-L1 blockade together with vaccine therapy facilitates effector T-cell infiltration into pancreatic tumors. J. Immunother 38, 1–11 (2015). [PubMed: 25415283]
27. Ha SJ, Mueller SN, Wherry EJ, Barber DL, Aubert RD, Sharpe AH, Freeman GJ, Ahmed R, Enhancing therapeutic vaccination by blocking PD-1-mediated inhibitory signals during chronic infection. J. Exp. Med 205, 543–555 (2008). [PubMed: 18332181]
28. Chea LS, Amara RR, Immunogenicity and efficacy of DNA/MVA HIV vaccines in rhesus macaque models. Expert Rev. Vaccines 16, 973–985 (2017). [PubMed: 28838267]
29. Kwa S, Sadagopal S, Shen X, Hong JJ, Gangadhara S, Basu R, Victor B, Iyer SS, LaBranche CC, Montefiori DC, Tomaras GD, Villinger F, Moss B, Kozlowski PA, Amara RR, CD40L-adjuvanted DNA/modified vaccinia virus Ankara simian immunodeficiency virus (SIV) vaccine enhances protection against neutralizationresistant mucosal SIV infection. J. Virol 89, 4690–4695 (2015). [PubMed: 25653428]
30. Ahonen CL, Doxsee CL, McGurran SM, Riter TR, Wade WF, Barth RJ, Vasilakos JP, Noelle RJ, Kedl RM, Combined TLR and CD40 triggering induces potent CD8+ T cell expansion with variable dependence on type I IFN. J. Exp. Med 199, 775–784 (2004). [PubMed: 15007094]
31. Sanchez PJ, McWilliams JA, Haluszczak C, Yagita H, Kedl RM, Combined TLR/CD40 stimulation mediates potent cellular immunity by regulating dendritic cell expression of CD70 in vivo. J. Immunol 178, 1564 1572 (2007). [PubMed: 17237405]
32. Borducchi EN, Cabral C, Stephenson KE, Liu J, Abbink P, Ng'ang'a D, Nkolola JP, Brinkman AL, Peter L, Lee BC, Jimenez J, Jetton D, Mondesir J, Mojta S, Chandrashekar A, Molloy K, Alter G, Gerold JM, Hill AL, Lewis MG, Pau MG, Schuitemaker H, Hesselgesser J, Geleziunas R, Kim JH, Robb ML, Michael NL, Barouch DH, Ad26/MVA therapeutic vaccination with TLR7 stimulation in SIV-infected rhesus monkeys. Nature 540, 284–287 (2016). [PubMed: 27841870]
33. Barber DL, Wherry EJ, Masopust D, Zhu B, Allison JP, Sharpe AH, Freeman GJ, Ahmed R, Restoring function in exhausted CD8 T cells during chronic viral infection. Nature 439, 682–687 (2006). [PubMed: 16382236]
34. Harper J, Gordon S, Chan CN, Wang H, Lindemuth E, Galardi C, Falcinelli SD, Raines SLM, Read JL, Nguyen K, McGary CS, Nekorchuk M, Busman-Sahay K, Schawalder J, King C, Pino M, Micci L, Cervasi B, Jean S, Sanderson A, Johns B, Koblansky AA, Amrine-Madsen H, Lifson J, Margolis DM, Silvestri G, Bar KJ, Favre D, Estes JD, Paiardini M, CTLA-4 and PD-1 dual blockade induces SIV reactivation without control of rebound after antiretroviral therapy interruption. Nat. Med 26, 519–528 (2020). [PubMed: 32284611]
35. Chen M-L, Pittet MJ, Gorelik L, Flavell RA, Weissleder R, von Boehmer H, Khazaie K, Regulatory T cells suppress tumor-specific CD8 T cell cytotoxicity through TGF-β signals in vivo. Proc. Natl. Acad. Sci. U.S.A 102, 419–424 (2005). [PubMed: 15623559]
36. Nigam P, Velu V, Kannanganat S, Chennareddi L, Kwa S, Siddiqui M, Amara RR, Expansion of FOXP3+ CD8 T cells with suppressive potential in colorectal mucosa following a pathogenic simian immunodeficiency virus infection correlates with diminished antiviral T cell response and viral control. J. Immunol 184, 1690–1701 (2010). [PubMed: 20053943]
37. Goswami R, Nelson AN, Tu JJ, Dennis M, Feng L, Kumar A, Mangold J, Mangan RJ, Mattingly C, Curtis AD II, Obregon-Perko V, Mavigner M, Pollara J, Shaw GM, Bar KJ, Chahroudi A, De Paris K, Chan C, Van Rompay KKA, Permar SR, Analytical treatment interruption after short-term antiretroviral therapy in a postnatally simian-human immunodeficiency virus-infected infant rhesus macaque model. MBio 10, e01971 19 (2019). [PubMed: 31488511]
38. Conway JM, Perelson AS, Li JZ, Predictions of time to HIV viral rebound following ART suspension that incorporate personal biomarkers. PLOS Comput. Biol 15, e1007229 (2019). [PubMed: 31339888]
39. Pasternak AO, Grijsen ML, Wit FW, Bakker M, Jurriaans S, Prins JM, Berkhout B, Cell-associated HIV-1 RNA predicts viral rebound and disease progression after discontinuation of temporary early ART. JCI Insight 5, e134196 (2020).

40. Bender AM, Simonetti FR, Kumar MR, Fray EJ, Bruner KM, Timmons AE, Tai KY, Jenike KM, Antar AAR, Liu PT, Ho Y-C, Raugi DN, Seydi M, Gottlieb GS, Okoye AA, Del Prete GQ, Picker LJ, Mankowski JL, Lifson JD, Siliciano JD, Laird GM, Barouch DH, Clements JE, Siliciano RF, The landscape of persistent viral genomes in ART-treated SIV, SHIV, and HIV-2 infections. Cell Host Microbe 26, 73 85.e4 (2019). [PubMed: 31295427]
41. Nixon CC, Mavigner M, Sampey GC, Brooks AD, Spagnuolo RA, Irlbeck DM, Mattingly C, Ho PT, Schoof N, Cammon CG, Tharp GK, Kanke M, Wang Z, Cleary RA, Upadhyay AA, De C, Wills SR, Falcinelli SD, Galardi C, Walum H, Schramm NJ, Deutsch J, Lifson JD, Fennessey CM, Keele BF, Jean S, Maguire S, Liao B, Browne EP, Ferris RG, Brehm JH, Favre D, Vanderford TH, Bosinger SE, Jones CD, Routy J-P, Archin NM, Margolis DM, Wahl A, Dunham RM, Silvestri G, Chahroudi A, Garcia JV, Systemic HIV and SIV latency reversal via non-canonical NF-κB signalling in vivo. Nature 578, 160 165 (2020). [PubMed: 31969707]
42. Okoye AA, Hansen SG, Vaidya M, Fukazawa Y, Park H, Duell DM, Lum R, Hughes CM, Ventura AB, Ainslie E, Ford JC, Morrow D, Gilbride RM, Legasse AW, Hesselgesser J, Geleziunas R, Li Y, Oswald K, Shoemaker R, Fast R, Bosche WJ, Borate BR, Edlefsen PT, Axthelm MK, Picker LJ, Lifson JD, Early antiretroviral therapy limits SIV reservoir establishment to delay or prevent post-treatment viral rebound. Nat. Med 24, 1430–1440 (2018). [PubMed: 30082858]
43. Im SJ, Hashimoto M, Gerner MY, Lee J, Kissick HT, Burger MC, Shan Q, Hale JS, Lee J, Nasti TH, Sharpe AH, Freeman GJ, Germain RN, Nakaya HI, Xue H-H, Ahmed R, Defining CD8+ T cells that provide the proliferative burst after PD-1 therapy. Nature 537, 417–421 (2016). [PubMed: 27501248]
44. Ferrando-Martinez S, Moysi E, Pegu A, Andrews S, Nganou Makamdop K, Ambrozak D, McDermott AB, Palesch D, Paiardini M, Pavlakis GN, Brenchley JM, Douek D, Mascola JR, Petrovas C, Koup RA, Accumulation of follicular CD8+ T cells in pathogenic SIV infection. J. Clin. Invest 128, 2089–2103 (2018). [PubMed: 29664020]
45. He R, Hou S, Liu C, Zhang A, Bai Q, Han M, Yang Y, Wei G, Shen T, Yang X, Xu L, Chen X, Hao Y, Wang P, Zhu C, Ou J, Liang H, Ni T, Zhang X, Zhou X, Deng K, Chen Y, Luo Y, Xu J, Qi H, Wu Y, Ye L, Follicular CXCR5- expressing CD8+ T cells curtail chronic viral infection. Nature 537, 412–416 (2016). [PubMed: 27501245]
46. Leong YA, Chen Y, Ong HS, Wu D, Man K, Deleage C, Minnich M, Meckiff BJ, Wei Y, Hou Z, Zotos D, Fenix KA, Atnerkar A, Preston S, Chipman JG, Beilman GJ, Allison CC, Sun L, Wang P, Xu J, Toe JG, Lu HK, Tao Y, Palendira U, Dent AL, Landay AL, Pellegrini M, Comerford I, McColl SR, Schacker TW, Long HM, Estes JD, Busslinger M, Belz GT, Lewin SR, Kallies A, Yu D, CXCR5+ follicular cytotoxic T cells control viral infection in B cell follicles. Nat. Immunol 17, 1187–1196 (2016). [PubMed: 27487330]
47. Roberts ER, Carnathan DG, Li H, Shaw GM, Silvestri G, Betts MR, Collapse of cytolytic potential in SIV-specific CD8+ T cells following acute SIV infection in rhesus macaques. PLOS Pathog. 12, e1006135 (2016). [PubMed: 28036372]
48. Connick E, Mattila T, Folkvord JM, Schlichtemeier R, Meditz AL, Ray MG, McCarter MD, Mawhinney S, Hage A, White C, Skinner PJ, CTL fail to accumulate at sites of HIV-1 replication in lymphoid tissue. J. Immunol 178, 6975–6983 (2007). [PubMed: 17513747]
49. Wodarz D, Skinner PJ, Levy DN, Connick E, Virus and CTL dynamics in the extrafollicular and follicular tissue compartments in SIV-infected macaques. PLOS Comput. Biol 14, e1006461 (2018). [PubMed: 30335747]
50. Haran KP, Hajduczki A, Pampusch MS, Mwakalundwa G, Vargas-Inchaustegui DA, Rakasz EG, Connick E, Berger EA, Skinner PJ, Simian Immunodeficiency Virus (SIV)-specific chimeric antigen receptor-T cells engineered to target B cell follicles and suppress SIV replication. Front. Immunol 9, 492 (2018). [PubMed: 29616024]
51. Okoye A, in Conference on Retroviruses and Opportunistic Infections (CROI, 2021), vol. 43.
52. Petrovas C, Ferrando-Martinez S, Gerner MY, Casazza JP, Pegu A, Deleage C, Cooper A, Hataye J, Andrews S, Ambrozak D, Del R.o Estrada PM, Boritz E, Paris R, Moysi E, Boswell KL, Ruiz-Mateos E, Vagios I, Leal M, Ablanedo-Terrazas Y, Rivero A, Gonzalez-Hernandez LA, McDermott AB, Moir S, Reyes-Ter.n G, Docobo F, Pantaleo G, Douek DC, Betts MR, Estes JD, Germain RN, Mascola JR, Koup RA, Follicular CD8 T cells accumulate in HIV infection and can

kill infected cells in vitro via bispecific antibodies. Sci. Transl. Med 9, eaag2285 (2017). [PubMed: 28100833]

53. Abel K, Alegria-Hartman MJ, Rothaeusler K, Marthas M, Miller CJ, The relationship between simian immunodeficiency virus RNA levels and the mRNA levels of alpha/beta interferons (IFN-α/β) and IFN-α/β inducible Mx in lymphoid tissues of rhesus macaques during acute and chronic infection. J. Virol 76, 8433–8445 (2002). [PubMed: 12134046]
54. Bosinger SE, Li Q, Gordon SN, Klatt NR, Duan L, Xu L, Francella N, Sidahmed A, Smith AJ, Cramer EM, Zeng M, Masopust D, Carlis JV, Ran L, Vanderford TH, Paiardini M, Isett RB, Baldwin DA, Else JG, Staprans SI, Silvestri G, Haase AT, Kelvin DJ, Global genomic analysis reveals rapid control of a robust innate response in SIV-infected sooty mangabeys. J. Clin. Invest 119, 3556–3572 (2009). [PubMed: 19959874]
55. Jacquelin B, Mayau V, Targat B, Liovat AS, Kunkel D, Petitjean G, Dillies MA, Roques P, Butor C, Silvestri G, Giavedoni LD, Lebon P, Barre-Sinoussi F, Benecke A, Muller-Trutwin MC, Nonpathogenic SIV infection of African green monkeys induces a strong but rapidly controlled type I IFN response. J. Clin. Invest 119, 3544–3555 (2009). [PubMed: 19959873]
56. Cheng L, Yu H, Li G, Li F, Ma J, Li J, Chi L, Zhang L, Su L, Type I interferons suppress viral replication but contribute to T cell depletion and dysfunction during chronic HIV-1 infection. JCI Insight 2, e94366 (2017).
57. Dyavar Shetty R, Velu V, Titanji K, Bosinger SE, Freeman GJ, Silvestri G, Amara RR, PD-1 blockade during chronic SIV infection reduces hyperimmune activation and microbial translocation in rhesus macaques. J. Clin. Invest 122, 1712–1716 (2012). [PubMed: 22523065]
58. Okoye A, D. M.1 D, B.1 V-M, M.1 C, M.1 L, H.1 B, J.1 S, M.. K.1 A, S.1 H, S. G.2 D, N.3 C, J. D.4 L, S. R.5 L, L. J.1 P, in Conference on Retroviruses and Opportunistic Infections (Topic Antiviral Medicine, 2020), vol. 28 (1), pp. 483.
59. Velu V, Vanderford TH, Freeman GJ, Ahmed R, Amara RR, in Conference on Retroviruses and Opportunistic Infections (CROI) (Seattle, 2012).
60. Gay C, Hardy WD, https://clinicaltrials.gov/ct2/show/NCT03787095.
61. Kovacs JA, https://clinicaltrials.gov/ct2/show/NCT03367754.
62. Martinez-Picado J, https://clinicaltrials.gov/ct2/show/NCT03767465.
63. Nath A, Wiebold AM, https://clinicaltrials.gov/ct2/show/NCT03239899.
64. Rasmussen TA, Rajdev L, Rhodes A, Dantanarayana A, Tennakoon S, Chea S, Spelman T, Lensing S, Rutishauser R, Bakkour S, Busch M, Siliciano JD, Siliciano RF, Einstein MH, Dittmer DP, Chiao E, Deeks S, Durand C, Lewin SR, Impact of anti-PD-1 and anti-CTLA-4 on the Human Immunodeficiency Virus (HIV) reservoir in people living with HIV with cancer on antiretroviral therapy: The AIDS Malignancy Consortium 095 study. Clin. Infect. Dis ciaa1530 (2021).
65. Kwa S, Lai L, Gangadhara S, Siddiqui M, Pillai VB, Labranche C, Yu T, Moss B, Montefiori DC, Robinson HL, Kozlowski PA, Amara RR, CD40L-adjuvanted DNA/ modified vaccinia virus Ankara simian immunodeficiency virus SIV239 vaccine enhances SIV-specific humoral and cellular immunity and improves protection against a heterologous SIVE660 mucosal challenge. J. Virol 88, 9579–9589 (2014). [PubMed: 24920805]
66. Van Rompay KK, Greenier JL, Cole KS, Earl P, Moss B, Steckbeck JD, Pahar B, Rourke T, Montelaro RC, Canfield DR, Tarara RP, Miller C, McChesney MB, Marthas ML, Immunization of newborn rhesus macaques with simian immunodeficiency virus (SIV) vaccines prolongs survival after oral challenge with virulent SIVmac251. J. Virol 77, 179–190 (2003). [PubMed: 12477823]

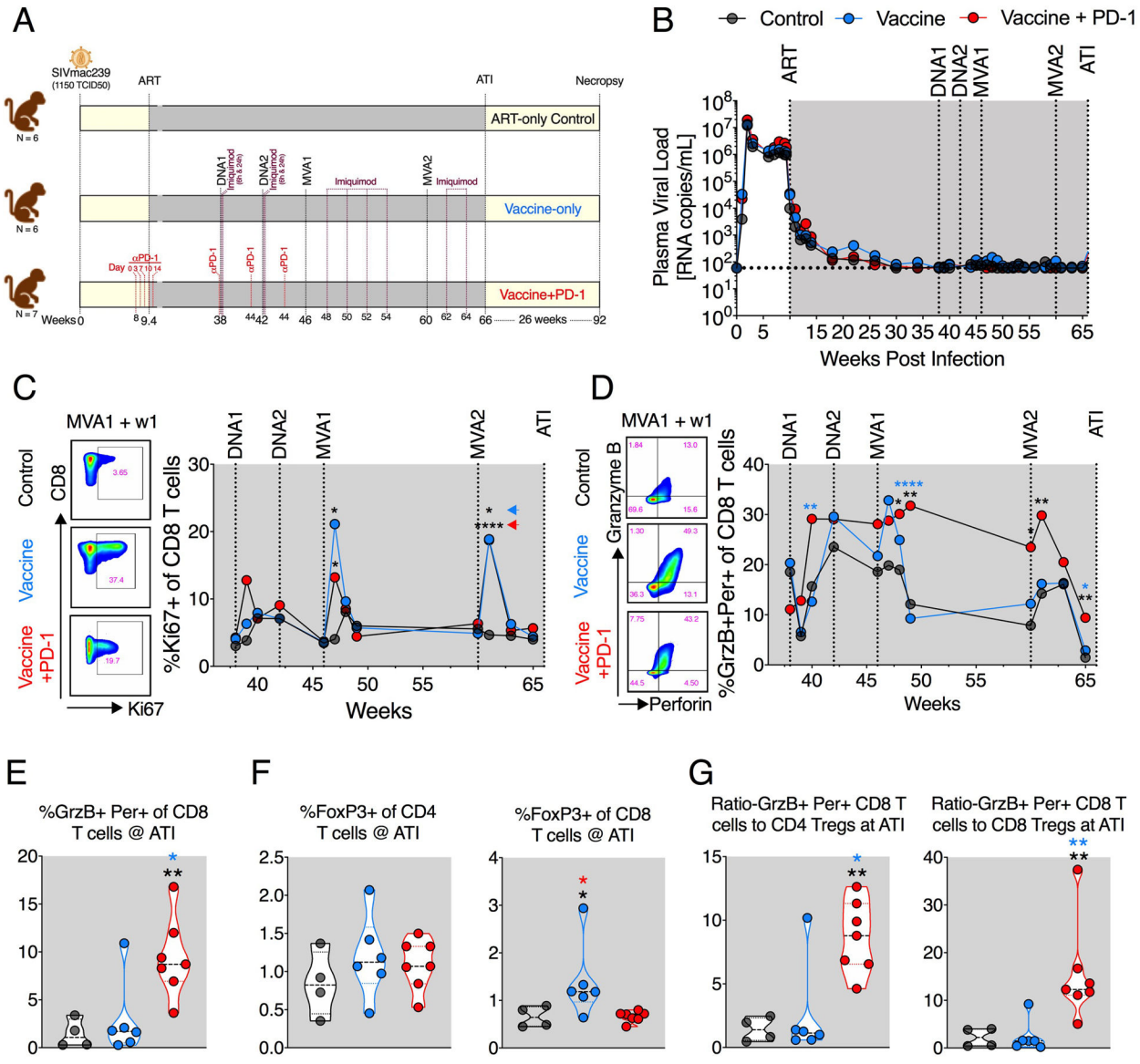

Fig. 1. PD-1 blockade combined with the DNA/MVA vaccination enhanced expression of cytolytic protein in CD8+ T cells.

(A) Schematic of the study design. (B) Viral suppression kinetics after infection and ART. Geometric mean values for each group are shown. (C and D) Frequency of proliferating (Ki67+) (C) and cytolytic (GrzB+ denoted as GrzB and perforin+ denoted as Per) (D) CD8+ T cells during the course of vaccination. (E) Cytolytic (GrzB+ Per+) CD8+ T cell frequencies at the time of ATI. (F) CD4+ and CD8+ Treg frequencies at ATI. (G) The ratio of Tregs and cytolytic CD8 T cells at ATI. The color of the significance star denotes the group to which comparison was made. Black/gray, blue, and red color refer to the control, vaccine, and vaccine + PD-1 groups, respectively. Colored arrowheads in (C) denote group to which significance star belongs. P value was calculated using Mann-Whitney test. W, weeks; ART, antiretroviral therapy; Per, perforin. *P ≤ 0.05; **P < 0.01; ****P < 0.0001.

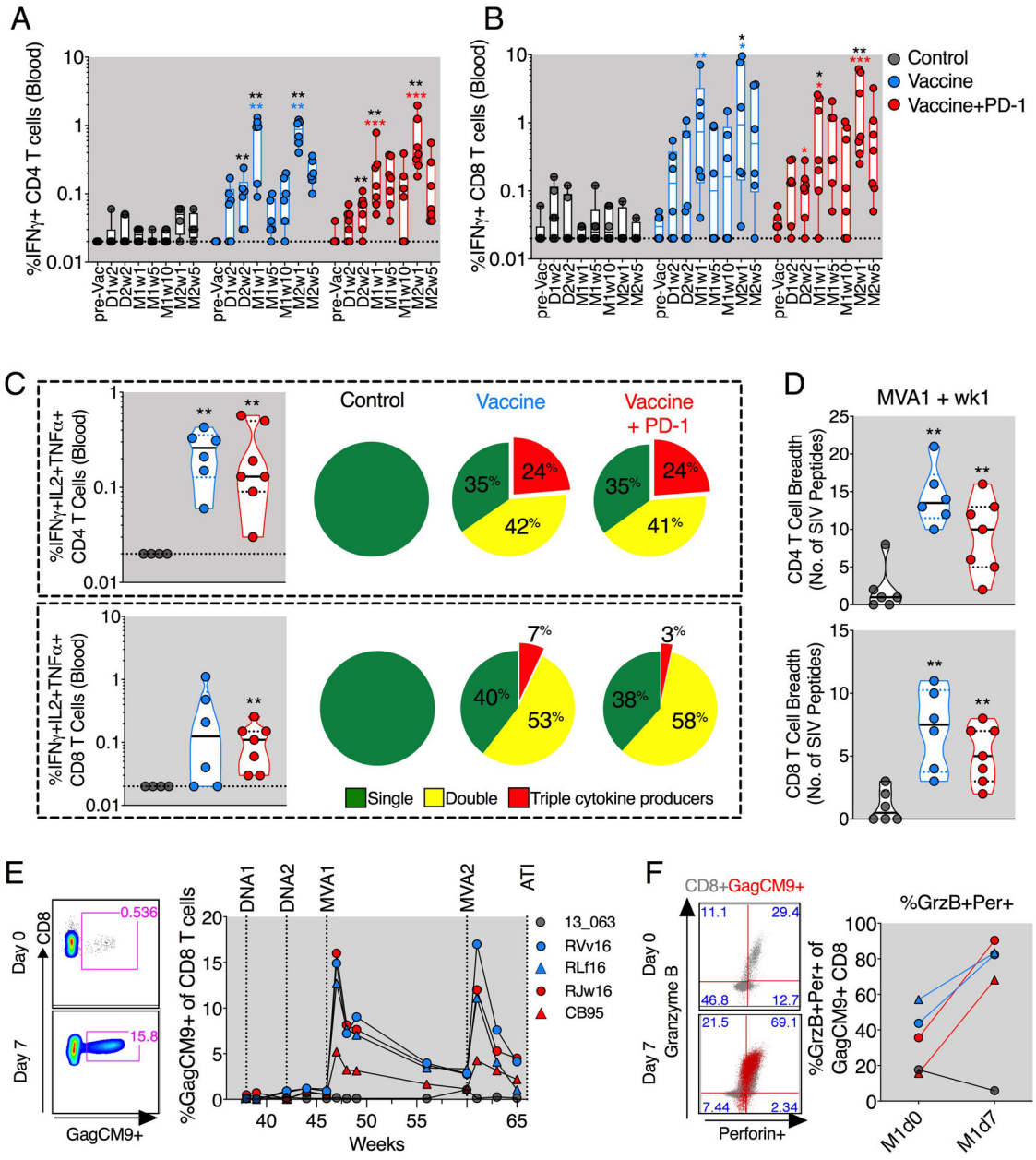

Fig. 2. DNA/MVA vaccination induced robust and highly functional SIV-specific CD4+ and CD8+ T cell responses in blood.

(A and B) Longitudinal analyses of SIV-specific IFNγ+ producing CD4+ (A) and CD8+ (B) T cells. (C) Frequency of triple cytokine (IFNγ+IL-2+TNFα+) producing T cells (scatter plots) and the proportion of T cells making single (IFNγ+ or IL-2+ or TNFα+), double (IFNγ+TNFα+/ IFNγ+IL-2+/IL-2+TNFα+), or triple (IFNγ+IL-2+TNFα+) cytokines in response to Gag and Env peptide stimulations (pie charts). (D) CD4+ and CD8+ T cell breadth defined by the number of SIV peptide minipools (Env and Gag) against which CD4+ and CD8+ T cells produced one or more IFNγ+/IL-2+/TNFα+ cytokines. (E) Frequency of SIV Gag-CM9 tetramer–specific CD8+ T cells. (F) Expression of GrzB and perforin on Gag-CM9 tetramer– specific CD8+ T cells before and after the first MVA

boost. The color of the significance star denotes the group to which comparison was made. Black/gray, blue, and red color refer to the control, vaccine, and vaccine + PD-1 groups, respectively. P value was calculated using Mann-Whitney test. D, DNA; M, MVA; W, week; pre Vac, prevaccination. *P ≤ 0.05; **P < 0.01; ***P < 0.001.

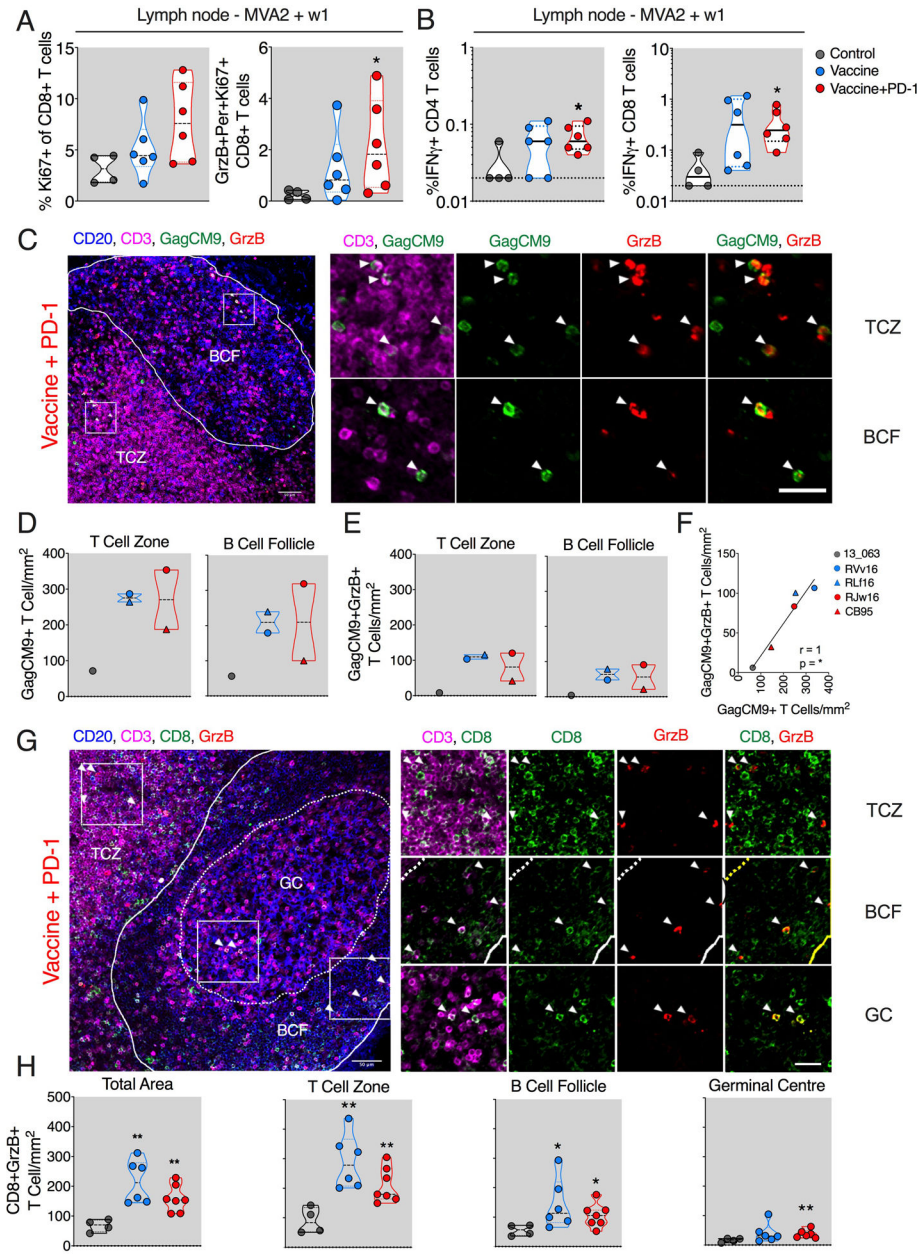

Fig. 3. DNA/MVA vaccination enhanced cytolytic CD8+ T cell localization in the LN.

(A) Frequencies of Ki67+ and GrzB+ Per+ Ki67+ CD8+ T cells. (B) SIV-specific IFNγ+ CD4+ and CD8+ T cell responses. (C to F) Quantification of total SIV Gag-CM9 tetramer–specific CD8+ T cells using in situ Gag-CM9 tetramer staining at week 1 of final MVA. Representative images from ~10 different regions of a LN section per animal (N = 2 for vaccine and vaccine + PD-1 groups and 1 for ART-only control group). (C) Summary of data for total GagCM9 tetramer+ (D) and for tetramer+ GrzB+ cells (E). (F) Spearman correlation between total GagCM9+T cell and GagCM9+GrzB+ T cell density. (G and H) Quantification of total CD8+ T cells coexpressing GrzB using immunohistochemistry. Representative image from ~10 different regions of a LN section per animal (N = 6 for vaccine and ART-only control groups and 7 for vaccine + PD-1 group) (G) and summary of

data for all animals (H). The inset (white square) shows the representative region picked to show zoomed images on the right. The color of the significance star denotes the group to which comparison was made. Black/gray, blue, and red color refer to the control, vaccine, and vaccine + PD-1 groups, respectively. P value was calculated using Mann-Whitney test. *P < 0.05; **P < 0.01. Scale bar, 25 μm.

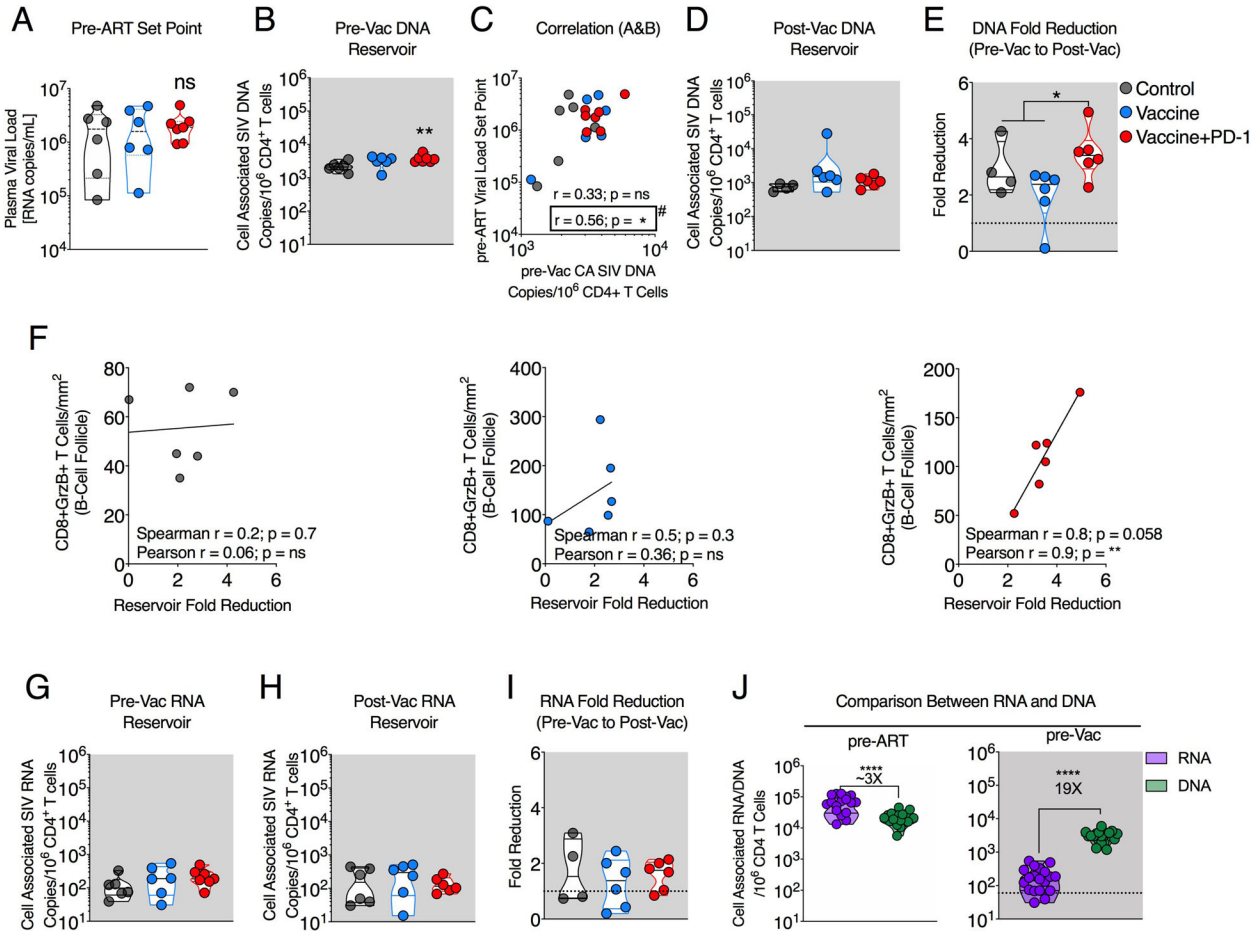

Fig. 4. PD-1 blockade combined with the vaccination reduced SIV reservoir under ART in LN.

(A) Pre-ART VL set point between ART-only control, vaccine-only, and vaccine + PD-1 group. ns, not significant. (B) Reservoir size (cell associated total SIV DNA per 106 CD4+ T cells) between control, vaccine, and vaccine + PD-1 groups at pre-Vac (week 16 after ART). (C) Spearman correlation between pre-ART VL set point and the SIV DNA reservoir at pre-Vac time point. (D) Reservoir size (cell-associated total SIV DNA per 106 CD4+ T cells) between control, vaccine, and vaccine + PD-1 groups at post-Vac (week 5 after final vaccination). (E) Reservoir fold reduction from pre-Vac to post-Vac time point. (F) Spearman correlation between fold reservoir reduction and CD8+GrzB+ T cell density inside BCF of the LN section at MVA2 + w1. Additional Pearson test showing significant correlation in vaccine + PD-1 group as indicated. (G to I) Transcriptionally active reservoir size (cell-associated total SIV RNA per 106 CD4+ T cells) between the control, vaccine, and vaccine + PD-1 groups at pre-Vac (week 16 after ART; G) and post-Vac (week 5 after final vaccination; H). (I) Fold reduction in SIV RNA from pre-Vac to post-Vac time points. (J) Comparison between the magnitude of cell associated total SIV RNA (purple; transcriptionally active reservoir) and DNA (green; total reservoir). The color of the significance star denotes the group to which comparison was made. Black/gray, blue, and red color refer to the control, vaccine, and vaccine + PD-1 groups, respectively. *P < 0.05; **P < 0.01; ****P < 0.0001.

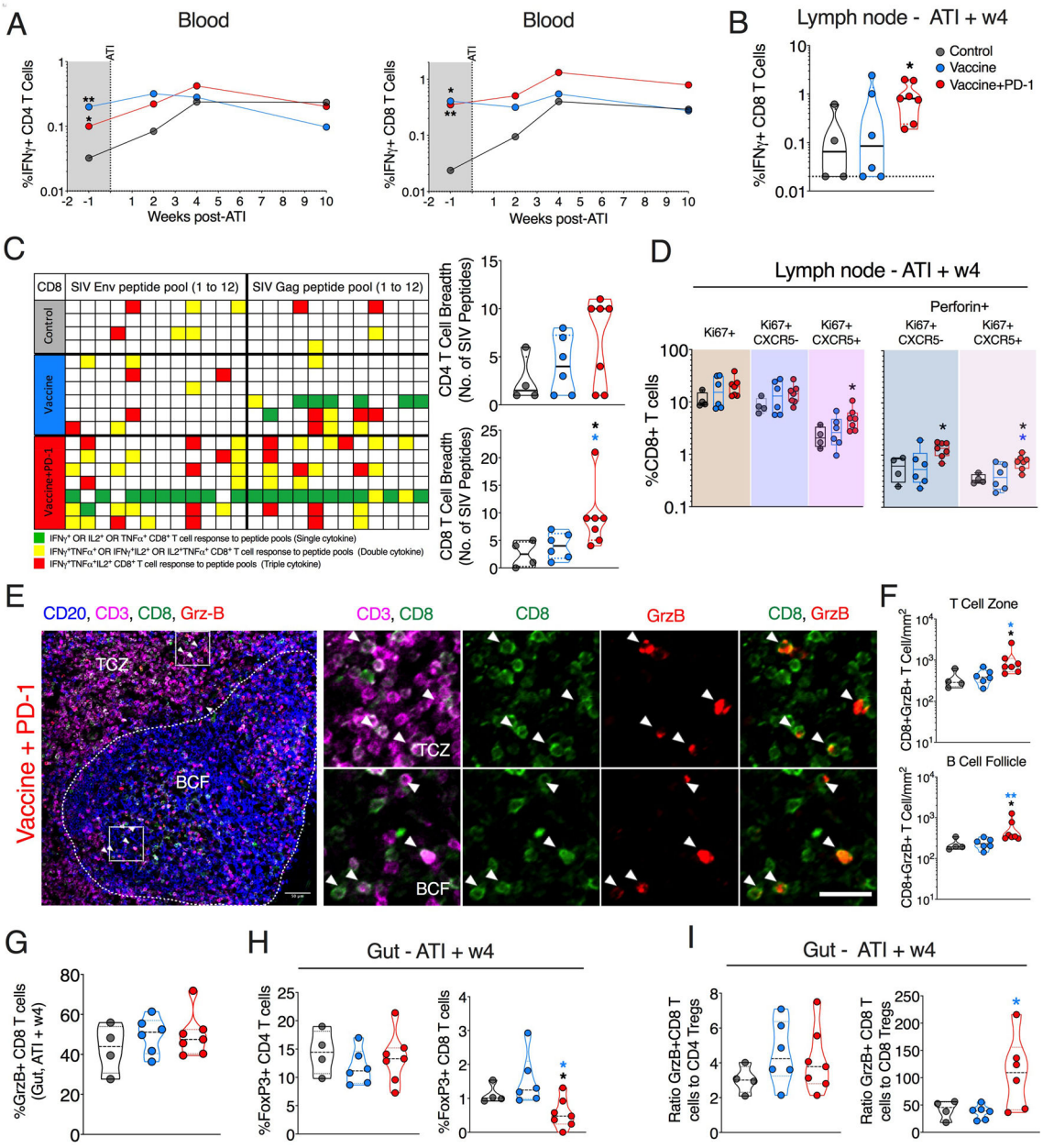

Fig. 5. PD-1 blockade combined with the vaccination preserved CD8+ T cell functional quality and breadth after ATI.

(A) Longitudinal SIV-specific IFNγ+ CD4+ and CD8+ T cells in blood. (B) SIV (Gag + Env)–specific IFNγ+ CD8+ T cell in response in LN. (C) CD8 T cell breadth against SIV Gag and Env peptide pools (grid plot) and the respective quantification for each group is shown on the right. (D) Frequency of total Ki67+, CXCR5− Ki67+, and CXCR5+ Ki67+ CD8+ T cells expressing perforin in LN at 4 weeks after ATI. (E and F) Quantification of total CD8+ T cells coexpressing GrzB using immunohistochemistry. Representative images from ~10 different regions of a LN section per animal (N = 6 for vaccine and ART-only control groups and 7 for vaccine + PD-1 group (E) and summary of data for all animals (F). The inset (white square) shows the representative region picked to show zoomed images

on the right. (G) Frequency of GrzB+ CD8 T cells in the gut at 4 weeks after ATI. (H) Frequency of regulatory CD4 and CD8 T cells in the gut at 4 weeks after ATI. (I) The ratio of cytolytic CD8 T cells to regulatory CD4 and CD8 T cells. The color of the significance star denotes the group to which comparison was made. Black/gray, blue, and red color refer to the control, vaccine, and vaccine + PD-1 groups, respectively. P value was calculated using Mann-Whitney test. *$P \leq 0.05$; **$P < 0.01$. Scale bars, 25 μm.

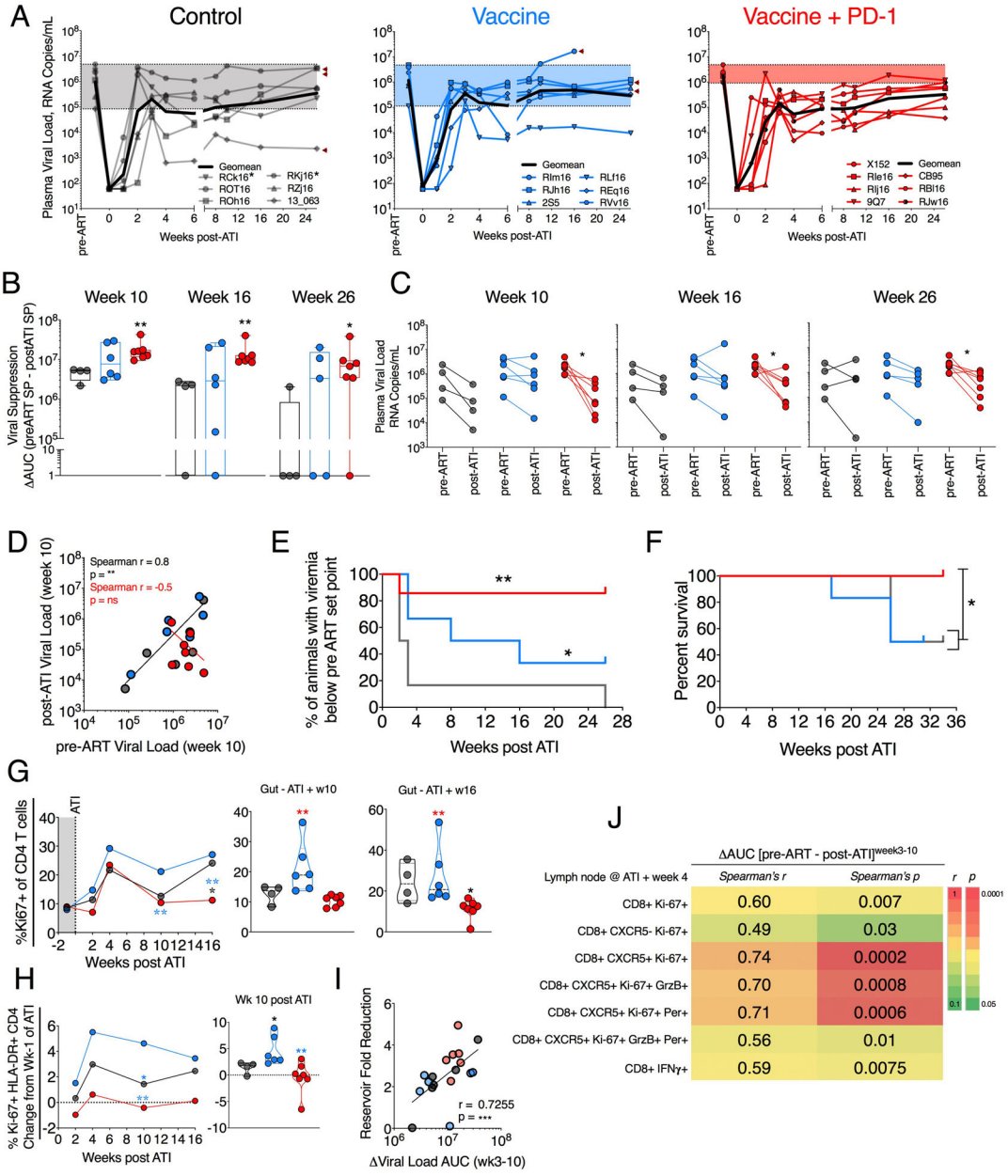

Fig. 6. PD-1 blockade combined with the vaccination significantly suppressed viral rebound after ATI and maintained lower CD4 T cell activation in gut.

(A) Viral rebound after ATI compared with pre-ART set point VL. The arrowheads indicate that animals died because of AIDS-related complications. Animals given MVA at week 60 in error are asterisked. (B) Viral suppression calculated as the difference between AUC of pre-ART (week 3 to week 10) set point viremia and post-ATI (week 3 to indicated week) set point viremia. (C) VL comparison between pre-ART set point and post-ATI viremia at weeks 10, 16, and 26. (D) Correlation of pre-ART VL with post-ATI VL shown at week 10 after ATI. (E) Kaplan-Meier curve showing percentage of animal controlling viremia twofold below pre-ART set point VL. (F) Kaplan-Meier curve showing percent animal survival without AIDS after ATI. (G) Ki67+ CD4 T cells after ATI. (H) Longitudinal change

in the frequency of Ki67+ HLA-DR+ CD4 T cells after ATI. (I) Spearman correlation between the fold SIV DNA reservoir reduction (pre- to postvaccination) and the viral suppression (VL AUC differences between pre-ART, weeks 3 to 10, and post-ATI, weeks 3 to 10 VL set points). (J) Spearman correlation between multiple CD8 T cell parameters and viral suppression (AUC differences) between pre-ART (weeks 3 to 10) and post-ATI (weeks 3 to 10) VL set points. For analyses in (A) to (H), P value was calculated using Mann-Whitney test. To adjust for seven multiple comparison in (I), we performed Bonferroni correction. Assuming the overall significance level to be 0.05, the significance threshold for individual correlation is 0.05/7 = 0.007. Under this significance threshold, four of seven are considered significant. The color of the significance star denotes the group to which comparison was made. Black/ gray, blue, and red color refer to the control, vaccine, and vaccine + PD-1 groups, respectively. *$P \leq 0.05$; **$P < 0.01$.